energies

MDPI

Article

Passive Cooling Analysis of an Electronic Chipset Using Nanoparticles and Metal-Foam Composite PCM: An Experimental Study

Faisal Hassan [1], Abid Hussain [1], Furqan Jamil [2], Adeel Arshad [3] and Hafiz Muhammad Ali [4,5,*]

[1] Mechanical Engineering Department, University of Engineering and Technology, Taxila 47050, Pakistan
[2] School of Engineering, Edith Cowan University, 270 Joondalup Drive, Joondalup, Perth, WA 6027, Australia
[3] Department of Mechanical and Construction Engineering, Faculty of Engineering and Environment, Northumbria University, Newcastle upon Tyne NE1 8ST, UK
[4] Mechanical Engineering Department, King Fahd University of Petroleum & Minerals, Dhahran 31261, Saudi Arabia
[5] Interdisciplinary Research Center for Renewable Energy and Power Systems (IRC-REPS), King Fahd University of Petroleum and Minerals, Dhahran 31261, Saudi Arabia
* Correspondence: hafiz.ali@kfupm.edu.sa

Abstract: Thermal management of electronic components is critical for long-term reliability and continuous operation, as the over-heating of electronic equipment leads to decrement in performance. The novelty of the current experimental study is to investigate the passive cooling of electronic equipment, by using nano-enriched phase change material (NEPCM) with copper foam having porosity of 97%. The phase change material of PT-58 was used with graphene nanoplatelets (GNPs) and magnesium oxide (MgO) nanoparticles (NPs), having concentrations of 0.01 wt.% and 0.02 wt.%. Three power levels of 8 W, 16 W, and 24 W, with corresponding heating inputs of 0.77 kW/m^2, 1.54 kW/m^2 and 2.3 kW/m^2, respectively, were used to simulate the heating input to heat sink for thermal characterization. According to results, at 0.77 kW/m^2 heating input the maximum base temperature declined by 13.03% in 0.02 wt.% GNPs-NEPCM/copper foam case. At heating input of 1.54 kW/m^2, the maximum base temperature reduction of 16% was observed in case of 0.02 wt.% GNPs-NEPCM/copper foam and 13.1% in case of 0.02 wt.% MgO-NEPCM/copper foam. Similarly, at heating input of 2.3 kW/m^2, the maximum temperature of base lessened by 12.58% in case of 0.02 wt.% GNPs-NEPCM/copper foam. The highest time to reach the set point temperature of 50 °C, 60 °C, and 70 °C was in case of GNPs-NEPCM/copper foam composites, while at all power levels MgO-NEPCM/copper foam gave comparable performance to GNPs based composite. Similar trend was observed in the study of enhancement ratio in operation time. From the results, it is concluded that the copper foam incorporation in NEPCM is an effective measure to mitigate the heat sink base temperature and can provide best cooling efficiency at low and higher heating loads.

Keywords: phase change materials; nanoparticles; metal foam; thermal management; electronic equipment

Citation: Hassan, F.; Hussain, A.; Jamil, F.; Arshad, A.; Ali, H.M. Passive Cooling Analysis of an Electronic Chipset Using Nanoparticles and Metal-Foam Composite PCM: An Experimental Study. *Energies* **2022**, *15*, 8746. https://doi.org/10.3390/en15228746

Academic Editor: Jude O. Iroh

Received: 27 September 2022
Accepted: 17 November 2022
Published: 21 November 2022

1. Introduction

With the advancement in electronic industry and miniaturization of electronic chipsets, the problem of high heat generation in electronic equipment has arisen, due to which the electronic equipment efficiency and life cycle are negatively influenced. Generally, the maximum allowable temperature for electronic chips to avoid damage due to overheating spans from 85 °C to 120 °C. For cooling of electronic equipment, various approaches are utilized like the use of thermal paste, air cooling, with fins, liquid cooling, nanofluids, heat pipes, vapor chamber, phase change material and porous media. The thermal energy storage material, i.e., PCM, is extensively researched for removing unwanted heat and keeping the temperature within acceptable limits in electronic cooling [1]. Active cooling

is typically used in nearly all equipment with a heat sink added to the circuit, but this method is insufficient to meet the demands of modern electronic equipment due to power consumption, noise, and poor performance. Passive cooling for steady and intermittent loads using a PCMs-based heat sink, on the other hand, has shown the ability to reduce peak temperatures and increase operating time within a given temperature range [2]. Researchers have explored the thermal optimization in PCMs by NPs, metal foams, shape stabilization, extruded surfaces, geometry variations, orientation variations in testing rigs, encapsulation, eutectic PCMs and heat pipes [3].

Iradukunda et al. [4] inspected the topology optimized heat sinks with sorbitol PCM for thermal evaluation for electronic equipment cooling. Results revealed that the topology optimized heat sink with PCM gave an enhancement factor of 3.5 in a temperature span of 50 °C to 100 °C, while the hybrid heat sink at cyclic heat input of 50 W lowered the peak temperature by 18.9 °C in comparison to baseline model. Mozafari et al. [5] studied the single and multiple PCM filled heat sinks for thermal control of electronic equipment. PCMs used in the study were RT44, n-Eicosane and RT58. According to results, the RT44 based heat sink gave least peak temperature and maximum melting period for single PCM case. Eicosane/RT44 PCM case enhanced the operational time from 3.3% to 12% compared to single RT44 or n-eicosane case. Rasool Kalbasi [6] investigated the PCM filled heat sink with forced convection. According to results, forced convection dissipated the PCM heat quickly to ambient, and hybrid heat sink performance at heat transfer coefficient of 50 $W/m^2/K$ was comparable to air cooled heat sink of 100 $W/m^2/K$. Xie et al. [7] studied the effect of natural convection on PCM packed heat sink using unique tree-shaped fins and conventional plate fins. The effects of parameters such as fin types, metal volume fraction, and orientations were studied for natural convection heat transfer. Results showed that the upward orientation resulted in better natural convection; increase in metal volume fraction negatively influenced the natural convection while improved conduction heat transfer, and tree shaped fins enhanced natural convection, hence heat transfer. Dammak and Hami [8] numerically optimized the PCM filled pin-fin heat sink for cooling of electronic equipment. The volume fraction of pin fin was 9% and pin-fin number was 72. Results showed that optimum design model took more time in latent heating phase, and highest temperature decline of 30% was obtained in comparison to the conventional model. Prasad et al. [9] investigated numerically the PCM based heat sinks under constant and variable load conditions. Under constant load conditions both conventional and PCM based heat sinks controlled the base temperature within the critical temperature, but under variable load conditions conventional heat sink failed to maintain the base temperature within SPT whilst the PCM based heat sink maintained the base temperature within set point temperature. Similarly, hybrid heat sinks further improved the thermal performance as it reduced the heat transfer coefficient by ten times less than that of the PCM based heat sink.

PCM have intrinsically low thermal conductivity, due to which heat transfer rate from PCM is low. The studies involving NPs for improving the thermal performance of PCMs for different applications are available in literature [10]. Farzanehnia et al. [11] investigated the paraffin/MWCNTs NEPCM for active and passive thermal control of electrical equipment. The use of NEPCM reduced solidification time by 6% than pure PCM, and enhancement ratio in operating times of 3.47 and 5.55 were obtained for NEPCM and PCM based cooling, respectively, in reaching the critical temperature of 60 °C for forced convection. Fan et al. [12] synthesized composite PCMs by combining 1-hexadecanol PCM with NPs of carbon nanotubes and GNPs in different fractions. The transient performance of a TES-based heat sink was investigated using the composite PCM. The use of carbon nanotubes was found to be detrimental because of reduced natural convection during the melting phase. However, the GNPs-based composite PCM enhanced the heat sink's transient thermal performance because it increased thermal conductivity and produced a minimal viscosity rise. Kothari et al. [13] investigated the finned/unfinned heat sinks with Al_2O_3 NPs for thermal management. The results revealed that for unfinned heat sinks with 2% NPs in PCM, operating time increased by 25%, while for one fin heat sinks with 4% NPs

in PCM, operating time increased by 28%. A 6% concentration of NPs in PCM decreased the latent heat of the PCM as well as the operating time. Pure PCM-based heat sink was recommended for higher set point temperatures. Joseph and Smith [14] explored the hybrid cooling using heat sink filled with graphene/paraffin NEPCM and forced convection. Thermal conductivity of PCM enhanced by 60% for 0.5 wt.% of graphene nanoparticles. Results indicated that the temperature reduction of 6 °C was attained for passive cooling using NEPCM mode under uniform heating load, and hybrid cooling resulted in energy savings up to 23%. Jalil et al. [15] explored the effect of PCM and NEPCM for enhancement of heat sink cooling performance. Experimentation was carried out by adjusting parameters such as with and without PCM, mold thickness of 30 mm and 60 mm, power inputs of 11 W, 13 W, and 15 W, and air flow rates of 1.5 m/s, 2.5 m/s, and 3.4 m/s. According to the findings, maximum temperature drop of 18 °C was noticed in the case of the 60 mm PCM mold, while 2% Al_2O_3 NPs concentration was considered to be appropriate for improving heat sink performance.

The thermal performance of PCMs is largely dependent on phase transition temperature and enthalpy value. Porous metal foams are being researched for improving the thermal response rate and to tackle the leakage issues of PCMs [16]. Marri et al. [17] explored the thermal behavior of heat sink loaded with PCM saturated in aluminum foam of varied porosity and PPI. It was observed that heat sink filled with PCM/metal foam gave enhancement ratio of 4.4 to reach a critical temperature. The uneven PPI (increasing from rear end to upper end) resulted in performance enhancement of 45% compared to uniform pore per inch foam case to reach a set point temperature. Venkateshwar et al. [18] studied n-octadecane PCM melting process under unidirectional pulsating thermal flux for different aluminum metal foam morphologies. Results indicated that the 15 °C surface temperature reduction and temperature fluctuation reduced by more than 20% with the positive gradient metal foam compared to uniform foam. Li et al. [19] prepared a slurry by introducing 20% mass concentration of nano-encapsulated PCM particles in water for passive thermal management. The nano encapsulated PCM consisted of paraffin core and polystyrene as shell, which was infiltrated into copper metal foam. Results showed that the maximum wall temperature reduction of 38% was observed in the case of metal foam embedded NEPCM compared to pure NEPCM. Zhao et al. [20] prepared a low melting alloy and coupled with carbon foam for the passive thermal control of electronic equipment. According to results, the low melting alloy extended the operating time by 1.5 times and lowered the heater temperature by 13.4 K, as compared to RT-60 paraffin case, during heating load condition. Arshad et al. [21] numerically studied the effects of various PCM composites for passive cooling of electronics. Copper nanoparticles of 1%, 3% and 5% volume fraction and copper, aluminum, nickel metal foams were inserted in heat sink. According to findings, the addition of 1% volume fraction of copper NPs along with copper metal foam enhanced the heat transfer rate by 8.12% and reduced the melting time duration by 18.10%. The NPs and metal foam based PCM composite presented lower heat sink base temperature while the increase in NPs volume fraction reduced the latent heating phase of PCM.

As literature indicates, the researchers have investigated pure PCMs and NEPCMs filled heat sinks, heat pipes or cavities for thermal control of electronic equipment. However, it is found that the research work involving the combined use of NPs and metal foam to thermally optimize PCMs for thermal control purposes is not available. The focus of the current study is to test the thermal management effectiveness of heat sink loaded with NEPCM/metal foam. Current experimental study utilized graphene nanoplatelets and magnesium oxide nanoparticles having non-metallic and metallic nature, respectively, with copper foam for thermal enhancement of PT-58 PCM. For the first time, the present study covers comparison of two nano-PCMs that include GNPs/PT-58 and MgO/PT-58 combined with copper foam for cooling of electronic equipment. Accordingly, the motive behind this study is specially focused on enhancing heat transfer rate and subsequently

cooling performance of heat sink to check the better configuration for base temperature reduction, the enhanced the operational time and increase the reliability of system.

2. Experimental Setup

The experimental setup consists of an aluminum heat sink with dimensions of 110 × 110 × 29 mm with a wall thickness of 4 mm. The heat sink is insulated with a fiber rubber block from all sides to prevent heat loss and allow for unidirectional heat flow from bottom to top. Heat sink is covered with a copper plate of 2 mm thickness, for improving heat dissipation rate. Silicon rubber fiberglass insulated heater (OMEGALUX SRFG-404/10-P-220V) of dimension 100 × 100 × 1.5 mm is used to imitate the heat generation by an electrical chipset and adhered at the rear end of heat sink by thermal paste. Pre calibrated 8 K type thermocouples (Omega, AWG-24, 0.5 mm wire diameter), temperature sensitivity between (−50 to 1350 °C) are inserted in various points in heat sink for temperature measurement. The thermocouple temperatures are recorded after every 5 s using Agilent (34972A) data acquisition unit. The silicon rubber heater is powered by DC power supply (Keysight Technologies 6675A) with a voltage range of 0–120 V and a current range of 0–18 A. To evaluate the thermal performance of heat sink, three heating inputs 0.77 kW/m^2, 1.54 kW/m^2, and 2.3 kW/m^2 (8 W, 16 W and 24 W) are opted which indicate the conventional power levels for operating electronic equipment with low to high power ratings. Ohm's law is applied for voltage estimation and a multimeter is used to measure the electrical power from DC supply. Before the start of experimentation, it was ensured that the heat sink temperature was retained at 28 °C. Schematic diagram and photographic view of the experimental setup are presented in Figures 1 and 2, respectively. The exploded view of heat sink assembly for present study in shown in Figure 3.

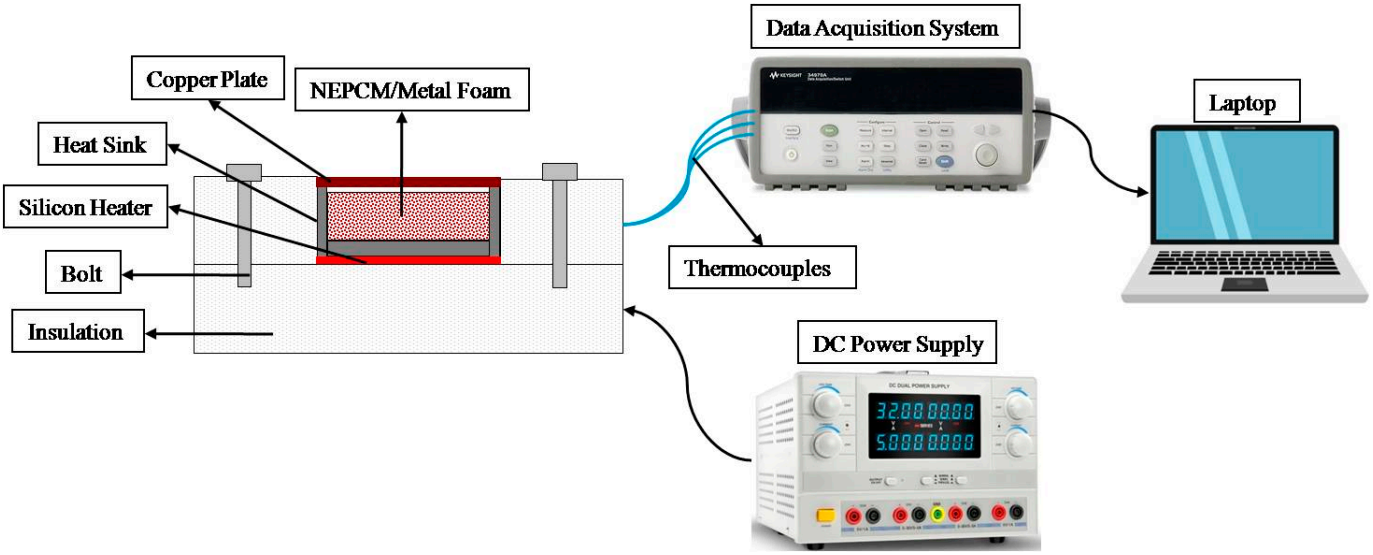

Figure 1. Schematic Diagram of Experimental Setup.

2.1. Materials

Paraffin wax PT-58 phase change material is utilized as latent heat storage material. The melting temperature of PT-58 was 58–60 °C as mentioned in literature [14]. Copper metal foam of dimensions 100 × 100 × 25 mm is employed as thermal conductivity enhancer. Thermophysical properties of PCM, copper metal foam, heat sink material (aluminum) and fiber rubber block are shown in Table 1. The heat sink cavity in empty and closed form is shown in Figure 4. The aim of adding highly conductive NPs in the base PCM is to augment the thermal conductivity of PCM and to improve the cooling efficiency of heat sink [22].The increase in the value of "k" of NEPCM mainly relies on size, type and concentration of NPs. The appropriate mixing of NPs in PCM improves the thermal

characteristics of base PCM. The two types of NPs utilized in the study are GNPs [23] and MgO NPs [24], and samples of NPs are shown in Figure 5 and TEM images are represented in Figure 6 (Courtesy: Advanced Chemical Supplier Material LLC [23]; Nanostructured and Amorphous Materials, Inc., Garland, TX, USA [24]). The thermophysical properties of NPs are mentioned in Table 2.

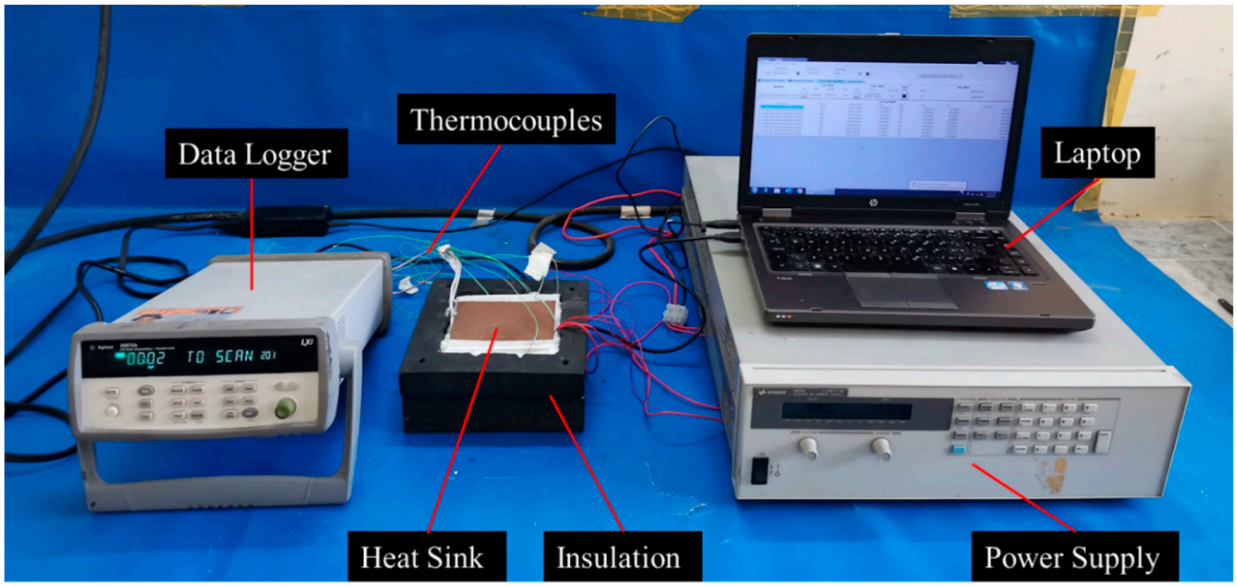

Figure 2. Photographic View of Experimental Setup.

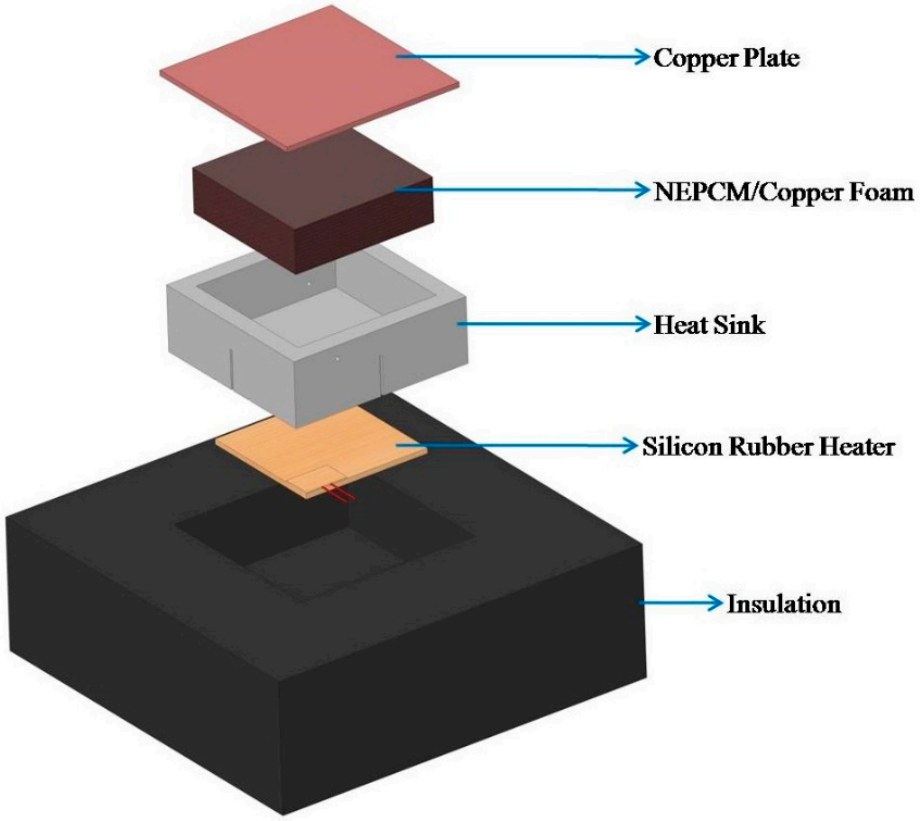

Figure 3. Exploded view of heat sink assembly.

Table 1. Thermophysical Properties of copper foam, PCM and heat sink material [14,25,26].

Property	Copper Foam	PT58 Pure PCM	Aluminum	Rubber Block
Melting point (°C)	1057	58–60	660.4	–
Thermal conductivity (W/m-K)	388	0.25 (Solid) 0.15 (Liquid)	237	0.043
Apparent density (Kg/m^3)	276	890 (Solid) 810 (Liquid)	2689	2500
Specific Heat (J/g°C)	0.383	2.47 (Solid) 2.71 (Liquid)	0.903	1.23
Heat storage capacity (kJ/kg)	–	225	–	–
Porosity (%)	97	–	–	–
Pore density (PPI)	35	–	–	–
Pore size (mm)	2.8	–	–	–

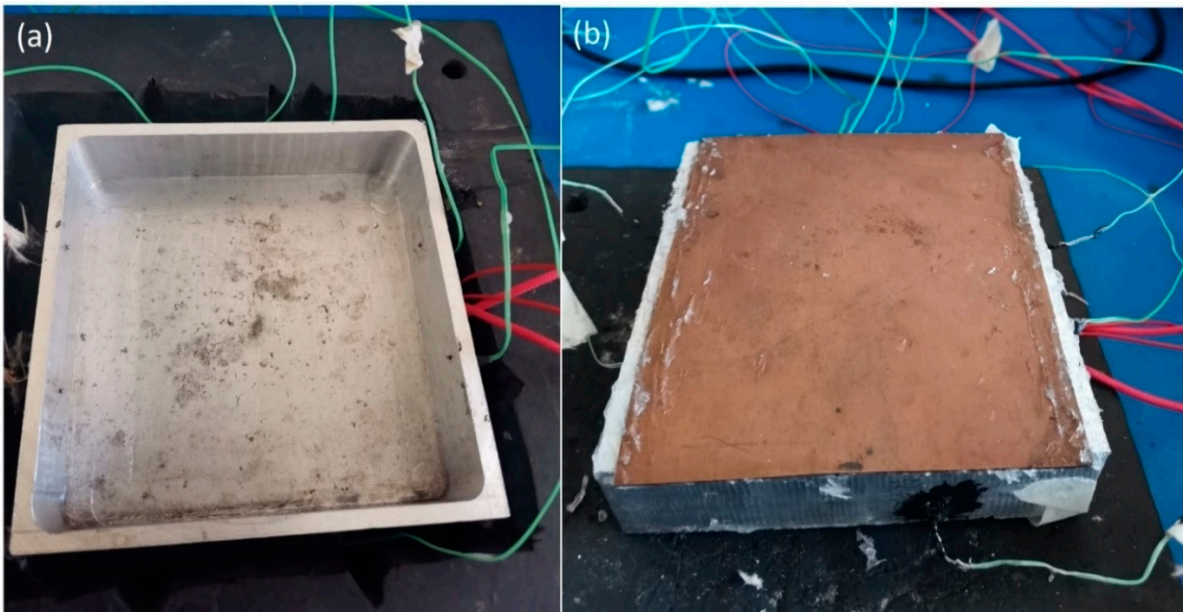

Figure 4. Aluminum heat sink cavity: (**a**) Empty form; (**b**) Closed form.

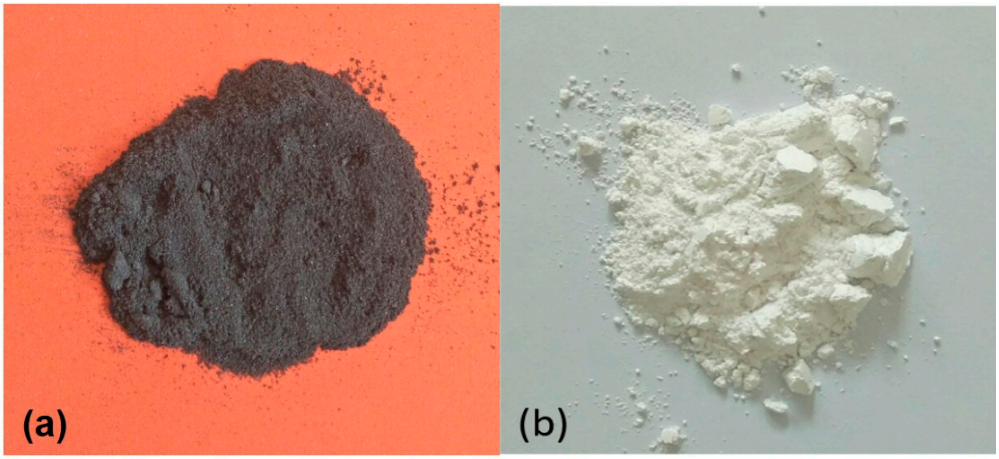

Figure 5. Sample photographs of: (**a**) Graphene nanoplatelets; (**b**) MgO NPs.

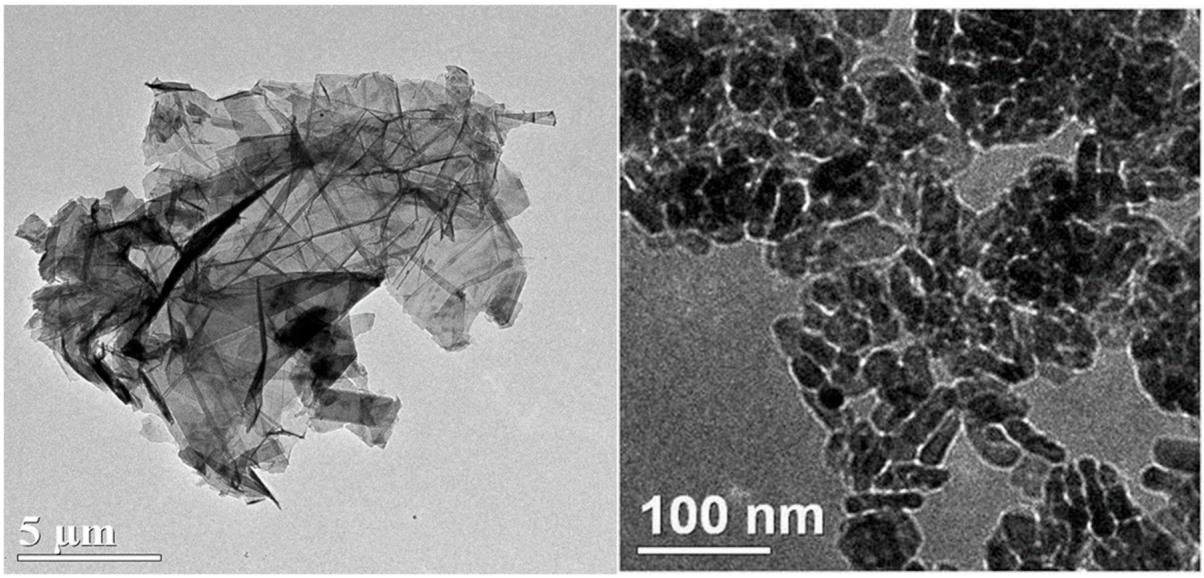

Figure 6. TEM images of GNPs [23] and MgO NPs [24].

Table 2. Nanoparticles Properties [23,24,27].

NP Type	GNPs	MgO
Color	Grey powder	White
Thermal conductivity	3000 (W/m K)	49.5 (W/m K)
Particle size	2–7 µm	20 nm
Thickness	2–10 nm	-
Specific surface area	20–40 m^2/g	50 m^2/g
Bulk density	0.10 g/cm^3	0.1–0.3 g/cm^3
Purity	>99%	99%
Morphology	Platelets morphology	Spherical

2.2. NEPCM Preparation and Saturation in Metal Foam

In this study, NEPCM and metal-foam/NEPCM composite temperature profiles are explored for the thermal control of electronic equipment. PT-58 PCM is utilized in this study owing to its optimum melting temperature range and high latent heat storage capacity. GNPs and MgO NPs are used to prepare the NEPCM. The NEPCM is prepared by using a two-step method comprised of dispersal and solidification steps [28,29]. The concentrations of NPs explored in this study are 0.01 wt.% and 0.02 wt.% of PCM. Higher volume fractions of NPs are not employed in the study to avoid further increase in the effective viscosity and agglomeration of NPs. The weight of solid PCM and NPs was measured by digital analytical balance (Shimadzu ATY224). In preparation of NEPCM, PCM was first melted by heating on hot plate magnetic stirrer, maintained at 80 °C, and then NPs in various concentrations were mixed with the molten PCM. The PCM/NPs mixture was continuously blended at 1100 rpm on hot plate magnetic stirrer (Corning PC-420D) for 30 min, and then the surfactant Sodium dodecyl sulfate (SDS) was added to the mixture; the amount of SDS surfactant added was about one third of NP's concentration. Then the mixture went through ultra-sonication using probe sonicator (Hielscher UP400St) at 24 KHz for 30 min and temperature was retained over the melting point of PCM. The ultrasonication improved NPs solubility in PCM, removed agglomeration, broke the particles into the mixture, and dispersed the particles homogeneously. The synthesis procedure of the NEPCM is shown in Figure 7. Finally, the NEPCM suspension was poured into the porous copper metal foam

and cooled at room temperature to obtain the NEPCM/foam composite. The stability of prepared NEPCM samples was analyzed visually. The samples of GNPs and MgO NEPCM samples of 0.01 wt.% and 0.02 wt.% after preparation, after 30 min and in solid state, are displayed in Figures 8 and 9, respectively.

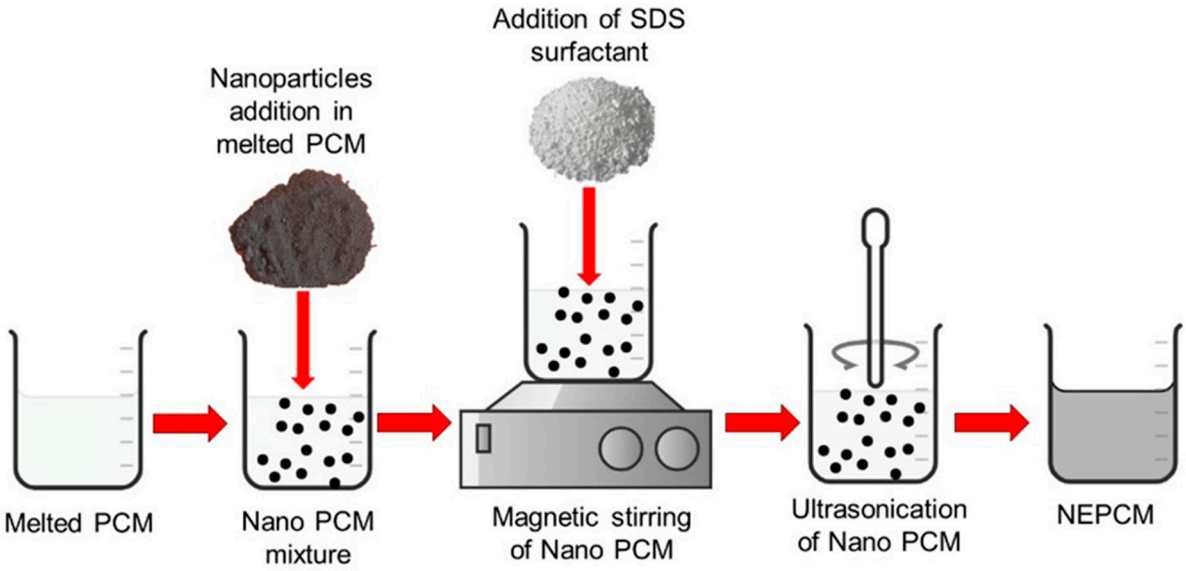

Figure 7. Schematic illustration of NEPCMs preparation.

Figure 8. GNPs samples: [0.01 wt.% (**a**) after preparation; (**b**) after 30 min; (**c**) in solid form]; [0.02 wt.% (**d**) after preparation; (**e**) after 30 min; (**f**) in solid form].

The melting temperature of each nano-PCM after adding NPs in base PCM is shown in Figure 10. It is clear that the melting temperature of GNPs/PCM based nano-PCM is reduced most as compared to other MgO/PCM and base PCM.

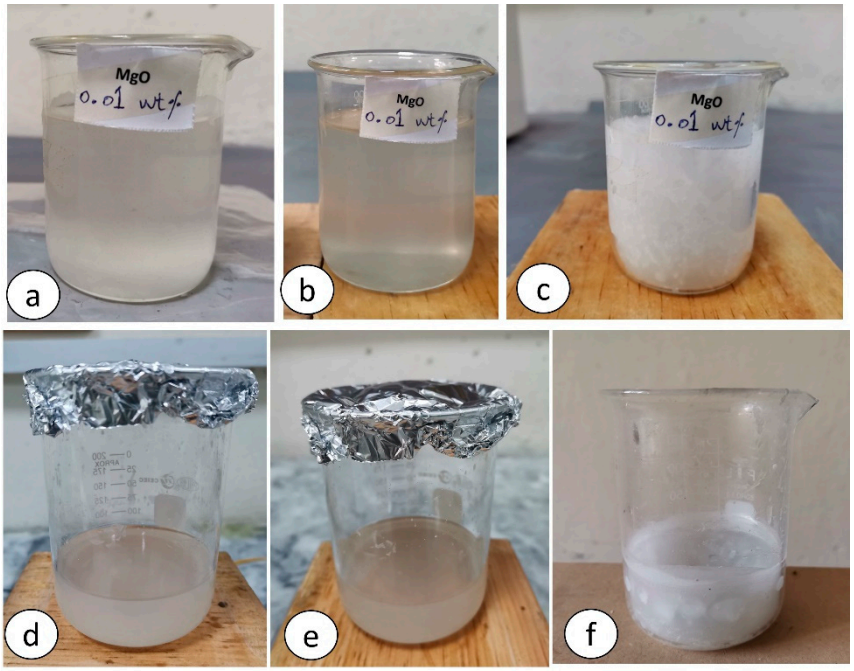

Figure 9. MgO samples: [0.01 wt.% (**a**) after preparation; (**b**) after 30 min; (**c**) in solid form]; [0.02 wt.% (**d**) after preparation; (**e**) after 30 min; (**f**) in solid form].

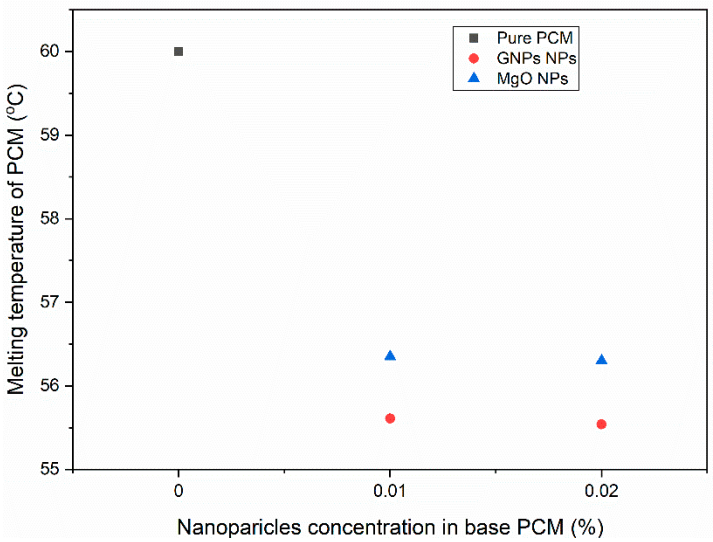

Figure 10. Melting temperature of PCM, GNPs/PCM based and MgO/PCM.

2.3. Thermocouples Positions

Highly sensitive and pre calibrated 8 K type thermocouples are positioned around the walls and base of the heat sink to analyze heat dissipation behavior of heat sink. The thermocouples are affixed to the heat sink sidewalls and base via 1 mm holes, using temperature-resistant epoxy adhesive to make them immovable and leakage proof. The positioning of thermocouples in heat sink is according to a previous study done on a heat sink of the same dimensions [30]. To measure the base temperature, two thermocouples T1, T2, 33.3 mm apart, are implanted in 3 × 1 mm^2 slots at the base of the heat sink. The thermocouples T3, T4 are positioned at 8 mm, T5, T6 positioned at 16 mm and T7, T8 positioned at 24 mm over the base of heat sink. For accurate temperature measurement within the heat sink, the thermocouples at the walls are implanted 20 mm inside the heat sink. The temperature was evaluated using the average temperature of two thermocouples

mounted at the same height during the experimentation, and the ambient temperature was kept at 28 °C. Table 3 presents the thermocouples positioning details. Figure 11 depicts the various isometric views of heat sink with thermocouple locations positioned inside heat sink.

Table 3. Location of thermocouples.

Name	T1, T2	T3, T4	T5, T6	T7, T8
Location of thermocouples	Heat sink base	8 mm	16 mm	24 mm

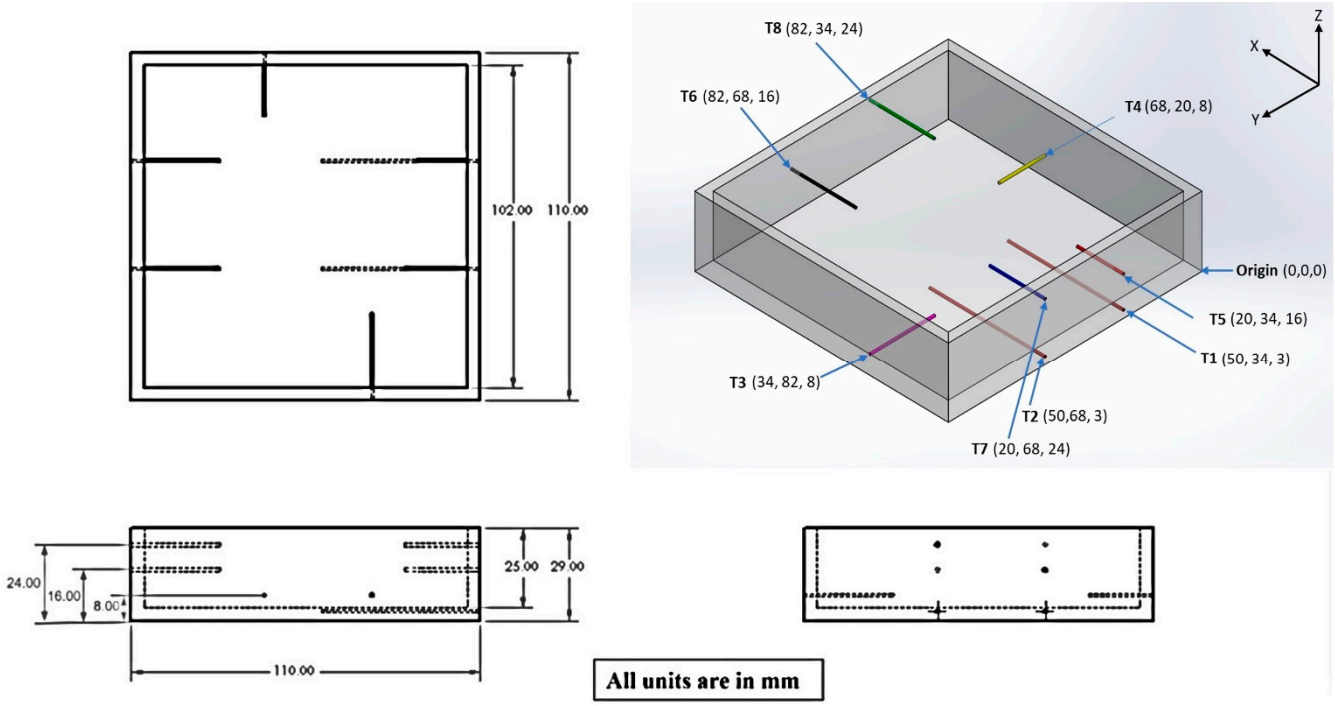

Figure 11. Various isometric views of heat sink depicting thermocouples positions.

2.4. Thermal Management Analysis

A comparison between 90 min charging and 90 min discharging of heat sink is conducted by employing different arrangements of heat sink, e.g., empty heat sink, PCM, PCM/copper foam (copper foam), NEPCM, NEPCM/copper foam packed heat sink. The thermal evaluation uses three power levels of 8 W, 16 W and 24 W. The heat sink is discharged in the same way as it is charged, with insulating sidewalls and base enabling one-dimensional heat flow from bottom to top for thermal analysis, and copper plate of 2 mm thickness covered the heat sink top to improve heat dissipation.

The cases considered for thermal management of heat sink are:

- 0.01 wt.% GNPs enhanced PT-58 (G1-NEPCM) with and without copper foam;
- 0.02 wt.% GNPs enhanced PT-58 (G2-NEPCM) with and without copper foam;
- 0.01 wt.% MgO enhanced PT-58 (M1-NEPCM) with and without copper foam;
- 0.02 wt.% MgO enhanced PT-58 (M2-NEPCM) with and without copper foam.

Enhancement Ratio in Operational Time

The enhancement ratio which indicates the increase in operational time duration of thermal system. It is presented by the fraction of time required by NEPCM and

NEPCM/copper foam enhanced heat sink to achieve a specific set point temperature to that of heat sink with no PCM and given by Equation (1):

$$\xi = \frac{t_{NEPCM,\ NEPCM/CF}}{t_{\ no\ PCM}} \tag{1}$$

2.5. Experimental Uncertainty Analysis

Uncertainty in experimentation happens as a result of either human or instrument inaccuracy. To guarantee that the results are valid, incorrect data can sometimes be recognized and eliminated promptly after analysis.

To estimate uncertainty in experimental parameters, Kline and McClintock [31] developed a root-sum-square combination for the individual variables. A variable can be expressed as Equation (2)

$$x = x_{measured} \pm \delta x \tag{2}$$

where,

x = final value of the variable;
$x_{measured}$ = measured value of variable;
δx = uncertainty in the value of measured variable due to fluctuation in the readings and scale of instrument.

The experimental findings x_R depend on various measured variables, each having distinct uncertainty value.

$$x_R = f(x_1\ ,\ x_2\ ,\ x_3\ ,\ \ldots\ldots\ x_n) \tag{3}$$

To estimate the uncertainty δx_R of resultant variable x_R, the expression given by Kline and McClintock [31] is,

$$\delta x_R = \sqrt{\left(\frac{\partial f}{\partial x_1}\delta x_1\right)^2 + \left(\frac{\partial f}{\partial x_2}\delta x_2\right)^2 + \ldots + \left(\frac{\partial f}{\partial x_n}\delta x_n\right)^2} \tag{4}$$

Equation (9) can be given as:

$$\frac{\delta x_R}{x_R} = \sqrt{(X_1\ \delta x_1)^2 + (X_2\ \delta x_2)^2 + \ldots + (X_n\ \delta x_n)^2} \tag{5}$$

where,

$$X_n = \frac{\partial f/\partial x_n}{x_R} \tag{6}$$

In the present scenario, the uncertainty in heating input is estimated as it is a crucial variable for heat sink thermal evaluation. Parameters concerning heating input are summarized as:

$$q = f(V,\ I,\ A) \tag{7}$$

where,

$$A = f(L,\ W) \tag{8}$$

Thus, Equation (9) is given as,

$$q = f(V,\ I,\ W, L) \tag{9}$$

The net fractional uncertainty of the heating input is evaluated by considering the uncertainties of employed voltage and current, as well as the length and width of the surface area as from Equation (10).

$$\frac{\delta q}{q} = \sqrt{X_v \delta V + X_I \delta I + X_W \delta W + X_L \delta L} \quad (10)$$

where

$$X_v = \frac{\frac{\partial q}{\partial V}}{q}; \qquad X_I = \frac{\frac{\partial q}{\partial I}}{q}; \qquad X_W = \frac{\frac{\partial q}{\partial W}}{q}; \qquad X_L = \frac{\frac{\partial q}{\partial L}}{q}$$

The symbols δV, δI, δW and δL are uncertainties in voltage, current, width and length of heat sink surface area, respectively. Investigations are done for highest and lowest heating input values. Uncertainties for current and voltage are gauged to be 0.015 and 3.1×10^{-8}, and for length and width of heating surface are 0.002 m and 0.0015 m, respectively. The current parameter has the highest level of uncertainty, accounting for about 80% of the total estimated uncertainty, whereas the voltage parameter has just a minor level of uncertainty. The highest and lowest uncertainties in heating input were calculated to be 6.91% and 4.5%, respectively. Furthermore, assessment is done three times on every value of heating input to assess the discrepancy of findings. The variation in findings was determined to be not more than 1.15% in any instance.

3. Results and Discussion

3.1. Validation of Experimentation Setup

Before scrutinizing the results, the experimental setup is verified by comparative analysis of an empty heat sink to those of prior studies conducted by Leong et al. [32] and Tariq et al. [33]. The validation of the current study is compared with the paper by Leong et al. [32], as the same trend can be seen from this reference paper. The Figure 6 in the reference paper of Leong et al. [32] has the same temperature trend with empty heat sink. The temperature variation in empty heat sink for Leong et al. [32] was around 26–55 °C, which is the same trend in the current research. Heat sink with inner dimensions of 102 × 102 × 25 mm and heating input of 8 W (0.77 kW/m^2) are used to relate the results. To validate the results, the same experimental protocols are maintained. From Figure 12 it can be noticed that the current study and prior studies present a close agreement. The deviation of 6 to 7% in temperature profile is due to difference in ambient conditions and heating input variations. As a result, further research is being conducted to assess the heat sink effectiveness under different scenarios.

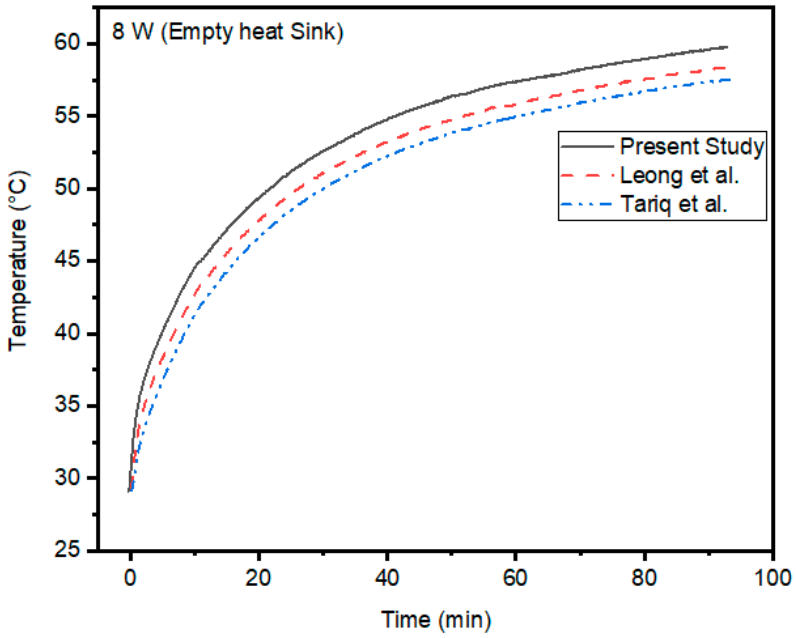

Figure 12. Validation of present experimental setup with the previous studies [32,33].

3.2. Results and Discussion

The thermal effectiveness of heat sink is estimated by applying various heating inputs (0.77 kW/m^2, 1.54 kW/m^2, 2.3 kW/m^2) at the base of heat sink by silicon rubber heater. The 90 min of charging and 90 min of discharging are considered to investigate the effect of different configurations of NEPCM and copper foam. The experimentation is done at a controlled environment temperature of 28 °C.

3.2.1. Base Temperature Comparison of Heat Sink with GNPs Composites

In this study, heat sink filled with PCM, NEPCM composites with 0.01 wt.% and 0.02 wt.% NPs is considered with and without copper foam. The heating inputs are varied to observe the influence of low to high heating loads on the different configurations of heat sink. The base of heat sink has two thermocouples, and the average value of these two thermocouples is used for baseline comparison of heat sink. The base temperature variations in heat sink filled with PCM, GNPs enhanced PCM, PCM and NEPCM incorporated in copper foam are presented in Figure 13. The dashed lines represent the transient temperature variations in heat sink packed with PCM and NEPCM while the solid lines represent the temperature variations in heat sink packed with PCM and NEPCM composites incorporated in copper foam.

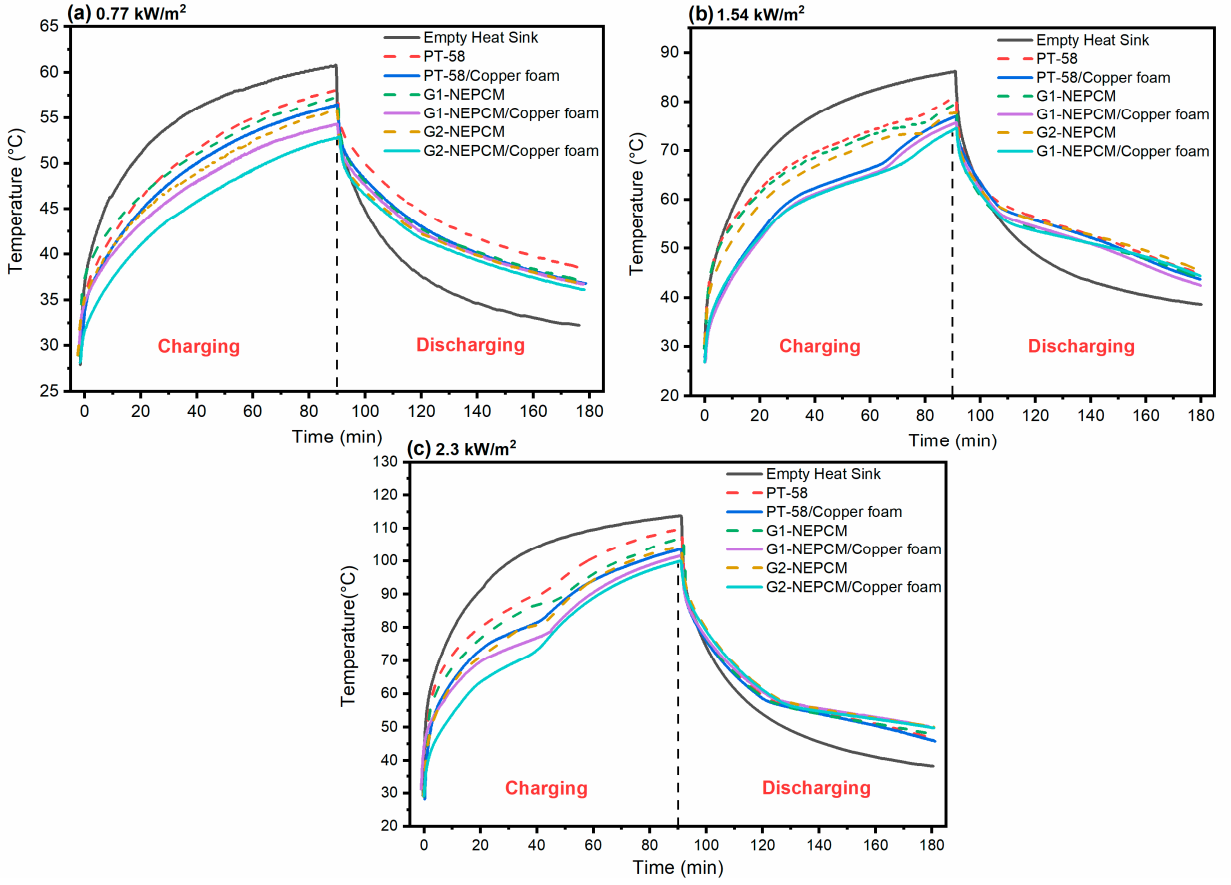

Figure 13. Charging and discharging analysis of various configurations of GNPs/PCM composites at heating inputs of: (**a**) 0.77 kW/m^2; (**b**) 1.54 kW/m^2; (**c**) 2.3 kW/m^2.

From Figure 13a, it is noted that when the empty heat sink reached the 60.77 °C temperature at the end of charging period for 0.77 kW/m^2, the maximum temperature reduction to 52.8 °C was observed in the case of G2-NEPCM/copper foam composite. The inclusion of PCM, G1-NEPCM and G2-NEPCM in heat sink lowered the base temperature by 2.65 °C, 3.49 °C and 4.87 °C, respectively. While the PCM/copper foam, G1-NEPCM/copper foam and G2-NEPCM/copper foam lowered the base temperature by 4.26 °C, 6.45 °C and 7.92 °C,

respectively. With the increase in concentration of NPs, the thermal responsiveness of PCM improved, with a moderate decrease in TES capacity, while the introduction of metal foam further enhanced the cooling performance of heat sink. For PCM and NEPCM composites, there was no phase change but only sensible heating until the end of charging period.

The Figure 13b shows the influence of heating input of 1.54 kW/m^2; at the completion of charging the empty heat sink reached a temperature of 86.2 °C, PCM lowered the temperature up to 5.1 °C, while the insertion of G1-NEPCM and G2-NEPCM lowered the base temperature by 6.45 °C and 7.82 °C. Similarly, the PCM/copper foam, G1-NEPCM/copper foam and G2-NEPCM/copper foam composites resulted in temperature reductions of 9.21 °C, 11.1 °C and 13.8 °C, respectively. The same trend further proves the fact that the copper foam is effective in improving heat sink performance as compared to NPs. The melting of PCM starts early in the case of metal foam, but the latent heating phase of PCM, NEPCM is enhanced due to metal foam. While in the case of PCM and NEPCM composites, the melting region is very small while after the latent heating phase a sharp increase in temperature profile can be observed, thus the viability of PCM is only before the latent heating is complete, but still the temperature of enhancement cases was much below the empty heat sink case.

To study the heat sink thermal behavior at high heating load, the heating input of 2.3 kW/m^2 was imparted, as depicted in Figure 13c. For empty heat sink case the temperature at the completion of the charging phase was 113.2 °C, and at the end of discharging temperature was 38.4 °C. At this power level, the introduction of PCM, G1-NEPCM and G2-NEPCM lowered the base temperature by 3.3 °C, 6.13 °C and 7.81 °C, respectively. Similarly, by filling heat sink with PCM/copper foam, G1-NEPCM/copper foam and G2-NEPCM/copper foam lessened the base temperature by 9.41 °C, 12.58 °C and 14.32 °C, respectively. The increase in NPs concentration in PCM lowered the base temperature, but the reduction was not much as at high heating load the NEPCM and NEPCM/copper foam composites completed their latent heating phase around 45 min of charging and underwent post-sensible heating. Similarly, at high heating load the stability of NPs in fully melted NEPCM started to deteriorate due to agglomeration and sedimentation, hence base temperature reduction was less effective.

The PCM and NEPCM composite with copper foam performance was much better than the simple PCM and NEPCM cases. Moreover, the discharging of NEPCM/copper foam composites was smoother than PCM and NEPCM cases. At the completion of the discharging phase, the empty heat sink achieved lower temperature than all cases due to the fact that heat transfer in the case of PCM composites is fast in the start, as PCM or NEPCM was in melting state, but slowed down after the PCM is solidified. The heat sink performance was mainly controlled by the melting behavior of PCM and NEPCM. In the case of PCM or NEPCM, the melting began at the bottom layer, which was in direct contact with the heat sink surface. Heat transfer in this layer was due to conduction, then further heat transfer in subsequent layers, not in direct contact with heat sink surface, took place by convection heat transfer. The inclusion of copper foam promoted the uniform heat transfer, as heat was transmitted by conduction within the copper foam. Due to conduction heat transfer in copper foam, the melting of PCM began early as compared to simple PCM or NEPCM cases. Then, due to natural convection, the melt fraction of PCM/NEPCM rose gradually until melting was complete. The main points of the above discussion can be summarized as:

- At heating input of 0.77 kW/m^2, the maximum temperature reduction of 13.03% was observed in the case of G2-NEPCM/copper foam as compared to empty heat sink. The discharing of NEPCM/copper foam case was better than that of simple PCM and NEPCM cases. The melting of PCM or NEPCM composites was not noticed in this case;
- For heating input of 1.54 kW/m^2, maximum temperature reduction was 16% for G2-NEPCM/copper foam, while for G2-NEPCM case temperature decline of 9.1% was obsered as compared to empty heat sink case. For NEPCM and NEPCM/copper foam

cases a sharp increase in temperature was noticed after the completion of the latent heating phase;

- At heating input of 2.3 kW/m^2, maximum base temperature was reduced by 12.48% and 6.89% for G2-NEPCM, with and without copper foam insertion. The increase in volume fraction of NPs from 0.01 to 0.02 wt.% improved the heat transfer rate in both cases of with and without copper foam.

3.2.2. Base Temperature Comparison of Heat Sink with MgO Composites

The influence of the introduction of MgO NPs in 0.01 wt.% and 0.02 wt.% in PCM with and without copper foam, at different heating loads, is given in Figure 14. MgO NPs thermal conductivity is lower as compared to GNPs, so the variations in heat sink thermal performance are observed. From Figure 14a, at the ending of charging process for 0.77 kW/m^2, maximum temperature reduction by the M1-NEPCM and M2-NEPCM was 3.75 °C, and 4.66 °C, respectively, while the temperature reduction in the case of M1-NEPCM/copper foam and M2-NEPCM/copper foam was 5.13 °C and 5.91 °C, respectively.

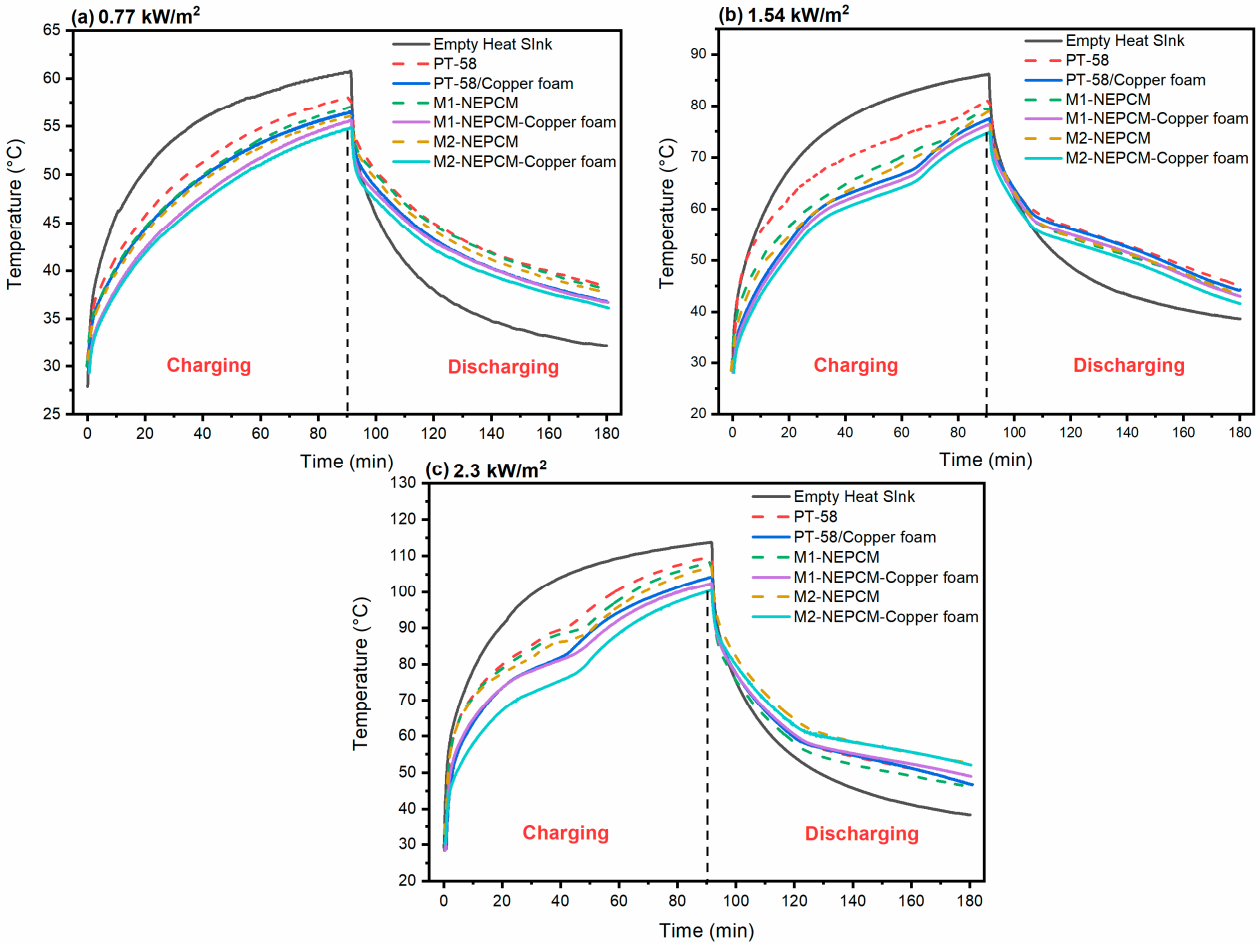

Figure 14. Charging and discharging analysis of various configurations of MgO/PCM composites at heating inputs of: (**a**) 0.77 kW/m^2; (**b**) 1.54 kW/m^2; (**c**) 2.3 kW/m^2.

In Figure 14b, at heating input of 1.54 kW/m^2, the heat sink with M1-NEPCM and M2-NEPCM reduced the base temperature by 6.22 °C and 7.18 °C, hence depicting much better performance than empty heat sink and PCM filled heat sink. For M1-NEPCM/copper foam and M2-NEPCM/copper foam cases, the base temperature lessened by 9.82 °C and 11.35 °C, respectively, as compared to empty heat sink. The performance of MgO composites can be examined at 40 min time duration, at which the empty heat sink reached 77 °C, while M1-NEPCM with and without copper foam reached about 61.72 °C and

64.72 °C, respectively, while M2-NEPCM, with and without copper foam, reached 60.28 °C and 63.26 °C, respectively.

At heating input of 2.3 kW/m^2, the case depicted in Figure 14c, the M1-NEPCM and M2-NEPCM dropped the heat sink base temperature by 4.81 °C and 6.04 °C, respectively, while M1-NEPCM/copper foam and M2-NEPCM/copper foam cases resulted in temperature reduction of 11.27 °C and 13.22 °C, respectively. At high heating input, the NEPCM/copper foam composite better performance was noticed, owing to high thermal conductivity of copper foam and increase in thermal response rate of PCM due to usage of both the MgO NPs and copper foam. The temperature profiles of different cases of heat sink revealed that the addition of NPs ensured a positive influence on heat transfer enhancement and base temperature reduction. For example, in case of M2-NEPCM at 24 W heating load and at 40 min of charging, the base temperature difference compared to empty heat sink was 19 °C, and for M2-NEPCM/copper foam the temperature difference was 28 °C. However, this trend is just up to complete melting of NEPCM, after melting phase sharp increase in temperature was noticed. The contours of temperature for the pure PCM, NEPCM, with and without copper foam, showed that the usage of copper foam lessened the heat sink base temperature and gave the homogenous temperature curve due to uniform heat transfer inside PCM and NEPCM. Some key points of the above discussion are:

- For a heating load of 0.77 kW/m^2, the maximum temperature of base was reduced by 9.7% and 7.6% for M2-NEPCM, with and without copper foam, respectively. At the end of discharging for NEPCM/copper foam composite gave lower temperature than simple NEPCM cases due to better heat dissipation rate.
- At heating input of 1.54 kW/m^2, maximum temperature of base was decreased by 11.38% and 13.38% for M2-NEPCM, with and without copper foam, respectively. The combined usage of MgO NPs and copper foam gave smooth PCM melting profile and offered lower base temperatures;
- Similarly, at heating input of 2.3 kW/m^2 for M2-NEPCM, with and without copper foam, temperature reduction of 11.62% and 5.3% was noticed. At high heating load, PCM was completely melted for both NEPCM and NEPCM/copper foam cases, thus increasing the heat sink base temperature considerably. The discharging at this load was better in the case of M2-NEPCM, with and without copper foam cases.

3.2.3. Spatial Variations in Temperature in Heat Sink

To explore the influence of temperature dispersion in heat sink at heating input of 2.3 kW/m^2, the two cases G2-NEPCM and M2-NEPCM/copper foam are employed; both cases are depicted in Figures 15 and 16, respectively. The base of heat sink with T1 and T2 thermocouples was taken as reference point, while the thermocouples T3, T4 and T5, T6 and T7, T8 were implanted at the height of 8 mm, 16 mm, and 24 mm, respectively, and positioned 20 mm inside the heat sink from the walls. The average value of two thermocouples was taken at the respective height to depict the spatial temperature variations inside heat sink. The area before the melting of PCM commences is pre-sensible heating region while the area after the melting of PCM is post-sensible heating. The temperature increase is sharp after the phase change heating area of the curve. The desired area of PCM is phase change heating, or latent heating region, during which the temperature increase is not sharp. From both figures it is noticed that the latent heating area is small in the case of G2-NEPCM, while for M2-NEPCM/copper foam case the latent heating region is more. The reason is that the PCM melting became smoother and more prolonged due to uniform heat distribution by copper foam. The copper foam hindered the convection heat transfer of NEPCM and promoted conduction heat transfer.

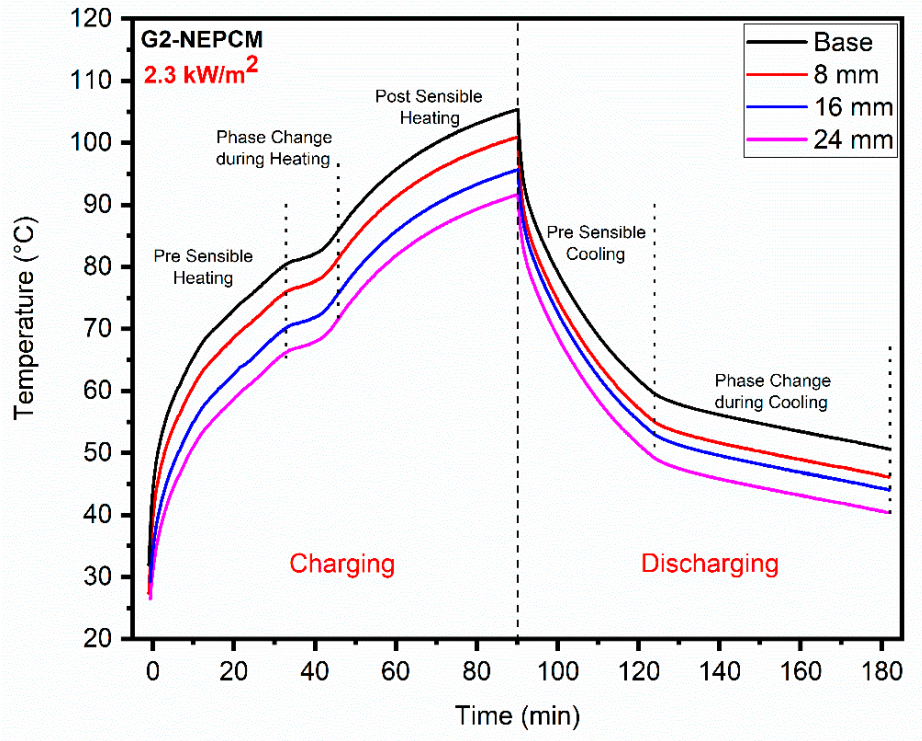

Figure 15. Spatial temperature distribution within heat sink filled with G2-NEPCM at 2.3 kW/m^2.

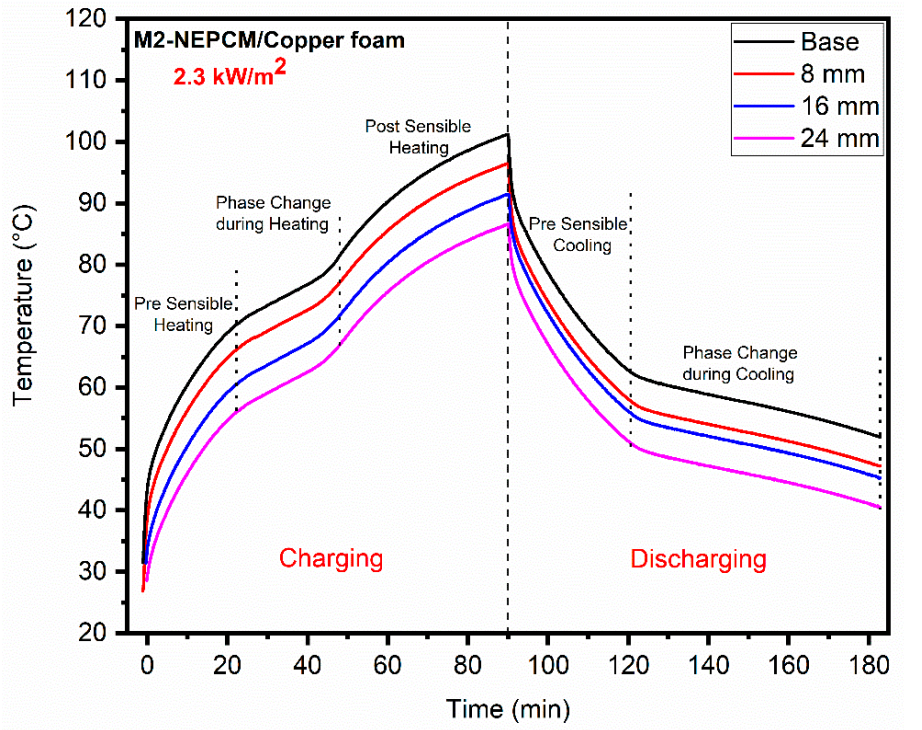

Figure 16. Spatial temperature distribution within heat sink filled with M2-NEPCM/copper foam at 2.3 kW/m^2.

The NEPCM is totally melted at the completion of the charging process, and when the discharging process begins, heat absorbed by melted NEPCM is promptly rejected during pre-sensible cooling phase. After about 30 min of discharging, the solidification of PCM starts, and then NEPCM slowly dissipates heat and at the end of discharging process PCM becomes completely solidified.

In both cases a considerable temperature difference is examined at the base of heat sink at various heights. A uniform temperature is observed to rise and fall in both charging and discharging cases for base, and at different heights inside the heat sink, the temperature profiles are uniform due to heat rejection of heat sink to the rubber block and top copper plate. Therefore, for improving heat transfer and cooling of heat sink, the thermal resistance should be minimal. The purpose of providing rubber block in this study is to provide controlled ambient conditions for uniform heat transfer from bottom of heat sink to top copper plate.

3.2.4. Effect of Different Heating Inputs on Heat Sink

To explore the influence of various heating inputs over the NEPCM/copper foam, two cases are illustrated which are G2-NEPCM with and without copper foam, and M2-NEPCM with and without copper foam. The base temperature variation in G2-NEPCM with and without copper foam is shown in Figure 17. For transient heating of heat sink at 0.77 kW/m^2 heating input the sensible heating took place, and NEPCM absorbed heat owing to latent heat capacity; the heat sink achieved a steady state temperature profile for both charging and discharging cases. While at heating load of 1.54 kW/m^2, the sharp increase in temperature can be observed during the first 20 min of charging, then the temperature increase rate slowed down before the complete melting of NEPCM. For heating input of 2.3 kW/m^2, the slope of temperature curve is small for NEPCM/copper foam case as compared to NEPCM case. At higher heating load due to complete melting of NEPCM, the temperature rises sharply till the end of charging process. Due to higher thermal conductivity of copper foam, employed with GNPs based NEPCM, the heat transfer rate of NEPCM enhanced, and higher heat dissipation rate from heat sink was achieved. The temperature contours NEPCM/copper foam showed the temperature reduction and temperature uniformity profile as compared to NEPCM cases.

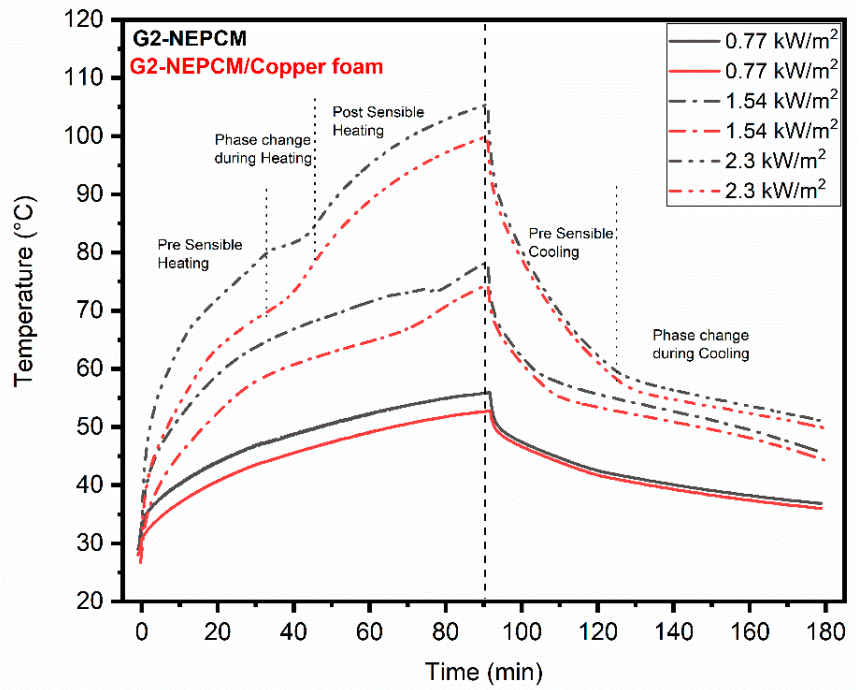

Figure 17. Charging and discharging curves for G2-NEPCM and G2-NEPCM/copper foam at different heating inputs.

The effect of different heating inputs on M2-NEPCM, with and without copper foam, is shown in Figure 18; the trends are similar to GNPs cases, but the temperature reduction in base is more prominent in the case of GNPs composites due to the higher thermal conductivity of GNPs.

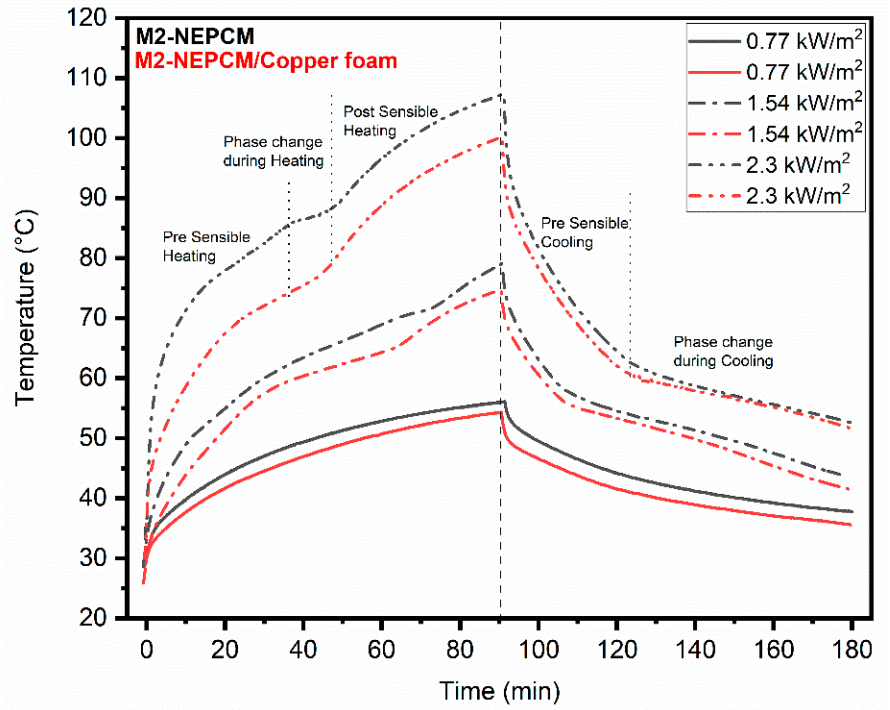

Figure 18. Charging and discharging curves for M2-NEPCM and M2-NEPCM/copper foam at different heating inputs.

Metal foam inclusion in PCM and NEPCM gave the best performance among the given approaches in both high and low heat generation rates. This comparison reveals that the use of metal foam can be the most effective way to improve the performance of the cooling performance of heat sink, as a significant reduction in baseline temperature was observed that was caused by the delay in PCM melting phase.

3.2.5. Analysis of Operational Time Variations for Various Target Temperatures

To explore the effect of various enhancements in heat sink, three target temperatures are selected to figure out the best possible configurations of heat sink. The Figure 19 presents the influence of introduction of NEPCM and NEPCM/copper foam in achieving the target temperature of 50 °C. For 8 W power level, the empty heat sink took only 17.4 min to reach the 50 °C, whereas heat sink filled with pure PCM took 33.05 min, and G2-NEPCM and M2-NEPCM took 45.07 min and 42.1 min, respectively, to achieve target temperature of 50 °C. Similarly, the G2-NEPCM/copper foam and M2-NEPCM/copper foam took 64.4 min and 52.42 min, respectively, to reach target temperature of 50 °C. At 16 W power level, NEPCM/copper foam composites took more time to reach 50 °C compared to NEPCM cases. Furthermore, at 24 W empty heat sink took only 1 min to reach 50 °C while G2-NEPCM/copper foam and M2-NEPCM/copper foam took 6.8 min and 4.3 min, respectively.

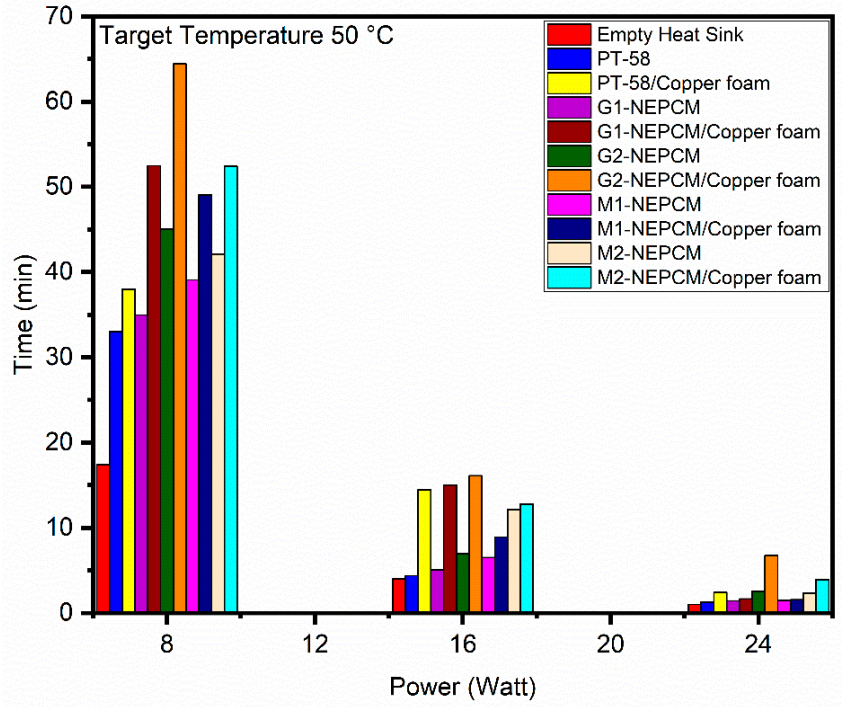

Figure 19. Time to attain target temperature of 50 °C for heat sink filled with PCM, NEPCM and NEPCM/copper foam composites.

To achieve the target temperature of 60 °C, Figure 20 shows the influence of various configurations of heat sink. At 8 W, the heat sink with enhancements did not achieve 60 °C temperature, at 16 W power level the empty heat sink took 11.5 min to achieve target temperature of 60 °C. The introduction of NPs in PCM increased the time to achieve the target temperature, but the increase was prominent for 0.02 wt.% of NPs. The heat sink packed with G2-NEPCM/copper foam took 46.1 min, and M2-NEPCM/copper foam took 38.98 min to achieve target temperature of 60 °C.

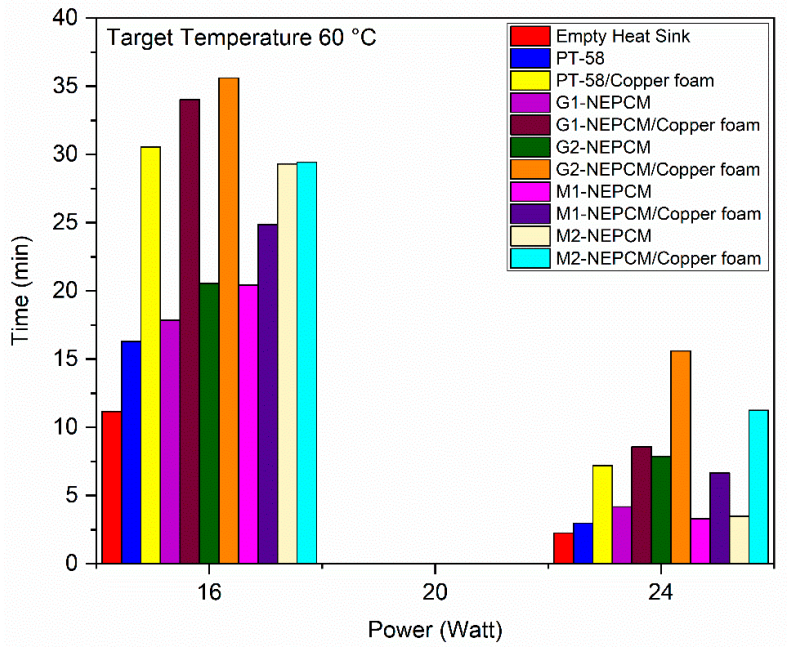

Figure 20. Time to attain target temperature of 60 °C for heat sink filled with PCM, NEPCM and NEPCM/copper foam composites.

Figure 21 demonstrates the influence of various enhancements in heat sink in attaining target temperature of 70 °C. At 16 W power level, empty heat sink took 23.4 min to reach 70 °C. The PCM and PCM/copper foam took 41 min and 69 min, respectively, to reach 70 °C. The NEPCM cases attained target temperature before the NEPCM/copper foam cases. The G2-NEPCM/copper foam took a maximum time of 78 min to attain 70 °C. For 24 W case, empty heat sink reached the target temperature in 5.7 min, G2-NEPCM/copper foam took 33.5 min to reach 70 °C temperature, while M2-NEPCM/copper foam reached target temperature in 24.94 min. Based on target temperature analysis of heat sink, the maximum time span was achieved in lower power level cases due to high heat absorption capacity of PCM, while at higher power levels, base temperature rose sharply due to complete melting of PCM and NEPCM.

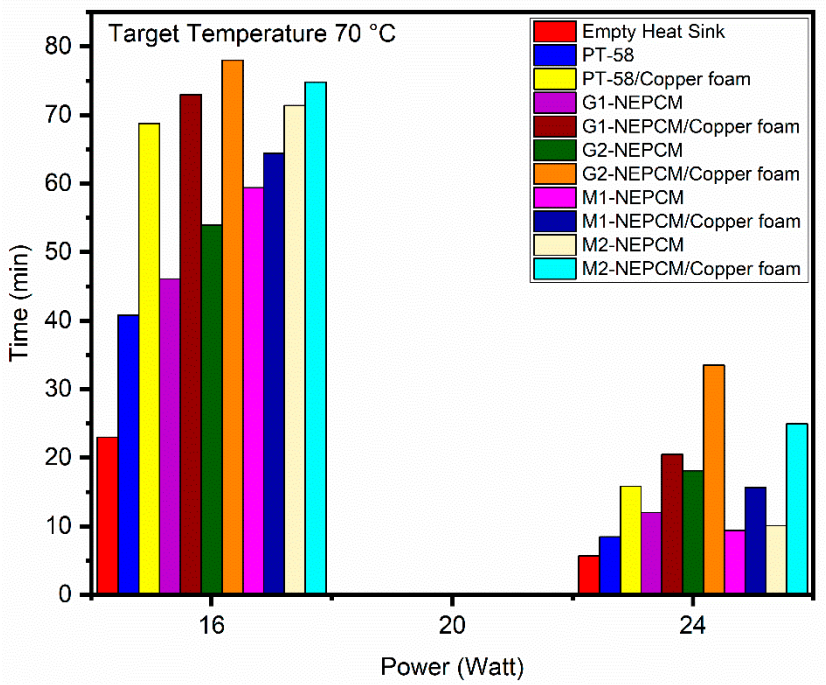

Figure 21. Time to attain target temperature of 70 °C for heat sink filled with PCM, NEPCM and NEPCM/copper foam composites.

The results indicated that the effect of copper foam was more significant even at high heating loads. From the target temperature figures, it is obvious that inclusion of metal foam offered significant improvement in heat transfer and base temperature reduction. Another notable phenomenon is the substantial lag in PCM or NEPCM latent heating phase with the porous copper foam, in comparison with the pure PCM or NEPCM cases. The cause for lag in melting was due to conduction heat transfer of copper foam inside solid PCM, which leads to more uniform temperature distribution through the PCM. As the result, the PCM or NEPCM took more time to complete the latent heating phase.

3.2.6. Enhancement Ratio in Operational Time for Various NEPCMs Composites

Enhancement ratio is defined as the ratio of time required to achieve a specific target temperature of heat sink filled with PCM/NEPCM composites to that of the empty heat sink. The enhancement ratio for various arrangements of heat sink is estimated at target temperatures of 50 °C, 60 °C and 70 °C. For target temperature of 50 °C case shown in Figure 22, G2-NEPCM/copper foam case gave maximum enhancement ratios of 3.7, 4 and 6.78 at 8 W, 16 W and 24 W, respectively. For M2-NEPCM/copper foam case, the enhancement ratio of 3.01, 3.2 and 3.94 was achieved at 8 W, 16 W and 24 W, respectively.

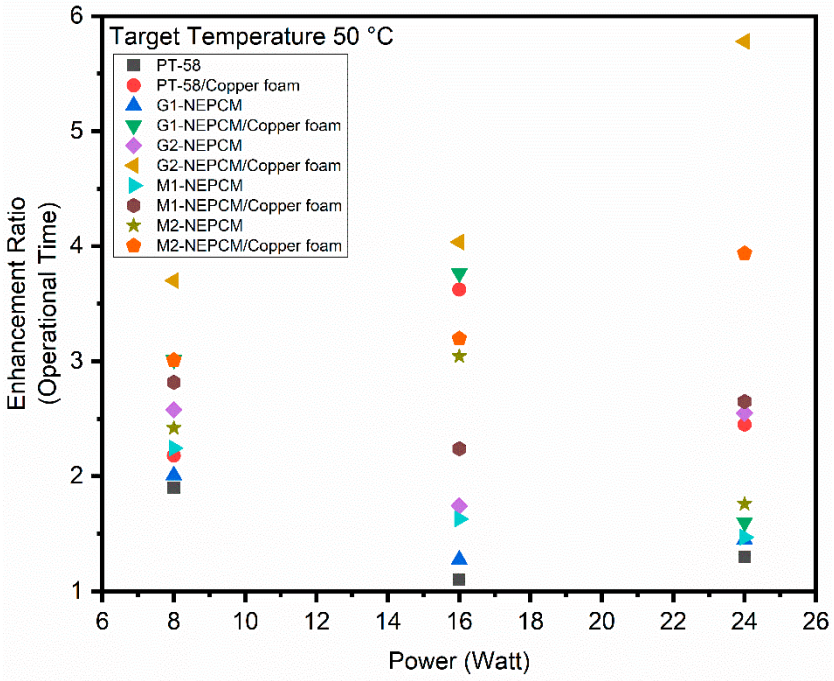

Figure 22. Enhancement ratios comparison for various heat sink configurations at operational time of 50 °C.

From Figure 23, for target temperature of 60 °C, maximum enhancement ratios of 3.2 and 6.9 were observed for G2-NEPCM/copper foam cases for 16 W and 24 W, respectively. Similarly, the enhancement ratio of 2.6 and 4.9 was noticed for M2-NEPCM/copper foam cases for 16 W and 24 W, respectively. The findings revealed that using NPs in PCM does not lead to positive effect on heat sink temperature decline, especially after complete melting. On the other hand, using copper foam in PCM and NEPCM showed the uniform heat transfer behavior as well as melting time enhancement.

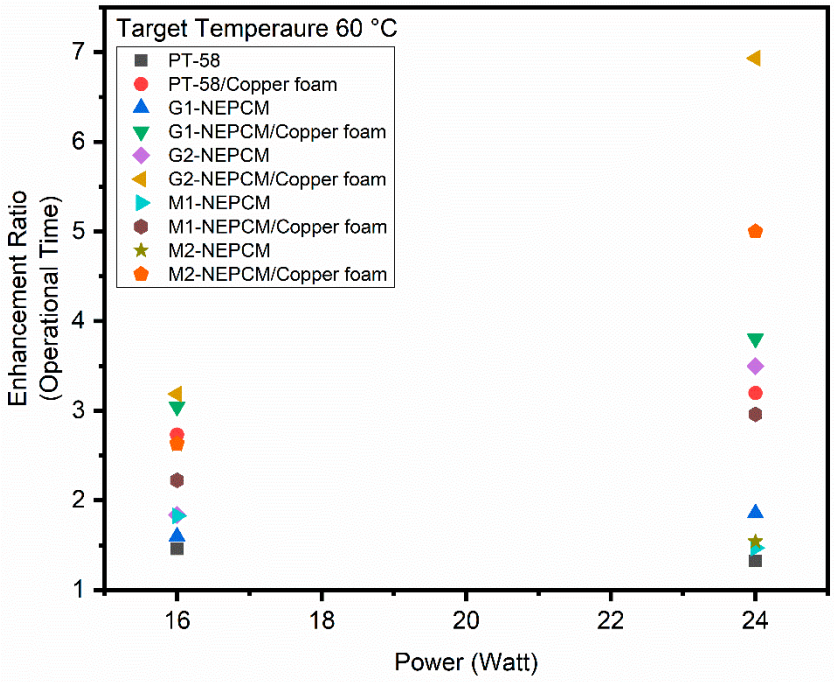

Figure 23. Enhancement ratios comparison for various heat sink configurations at operational time of 60 °C.

For target temperature of 70 °C shown in Figure 24, the G2-NEPCM/copper foam and M2-NEPCM/copper foam presented almost the same enhancement ratio at 16 W heating load. But for 24 W case, G2-NEPCM/copper foam gave enhancement ratio of 5.9, while M2-NEPCM/copper foam offered enhancement ratio of 4.1 in achieving the target temperature of 70 °C.

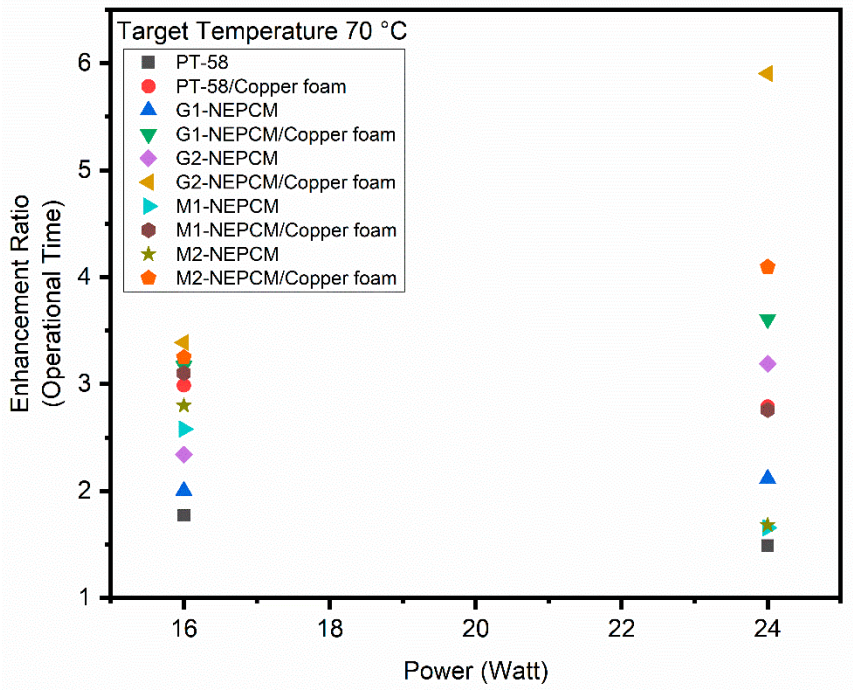

Figure 24. Enhancement ratios comparison for various heat sink configurations at operational time of 70 °C.

From the enhancement ratio study, it is obvious that the heat sink thermal performance is best in cases of NEPCM/copper foam composites, while the performance of NEPCM based heat sink is also better than other cases. The latent TES capacity of PCM is greater than the sensible heat capacity, due to which the contribution of the PCM in the heat transfer is contingent on the melting process. With the increase in NPs concentration, a slight TES capacity drop was noticed for PCM enhanced with GNPs and MgO. Charging performance was better when GNPs were used, compared to when MgO NPs were used.

3.3. Comparison of Experimental Results with the Literature

The studies utilizing PCMs, NEPCMs, PCM packed in metal foam for thermal management of electronic equipment, are available in the literature. The present study involved the thermal management of heat sink using GNPs and MgO NEPCM saturated with copper foam. The purpose of the study is to lower heat sink base temperature and enhance the optimal operating time duration. The comparison of the current study with the previous studies [11,34–40] (as shown in Figure 25) indicates the viability of NEPCM/copper foam composite. The present study gave better performance than most of the studies because of better thermal performance due to combined use of NEPCMs and copper foam. The maximum temperature reduction of 14.32 °C was observed in the case of G2-NEPCM/copper foam case, while from the literature the temperature reduction of 14 °C was noticed for the studies [36,40] which employed finned heat sinks with NEPCMs. The improvement in heat sink cavity, or the use of forced convection, can further improve the capacity of current study in terms of thermal management.

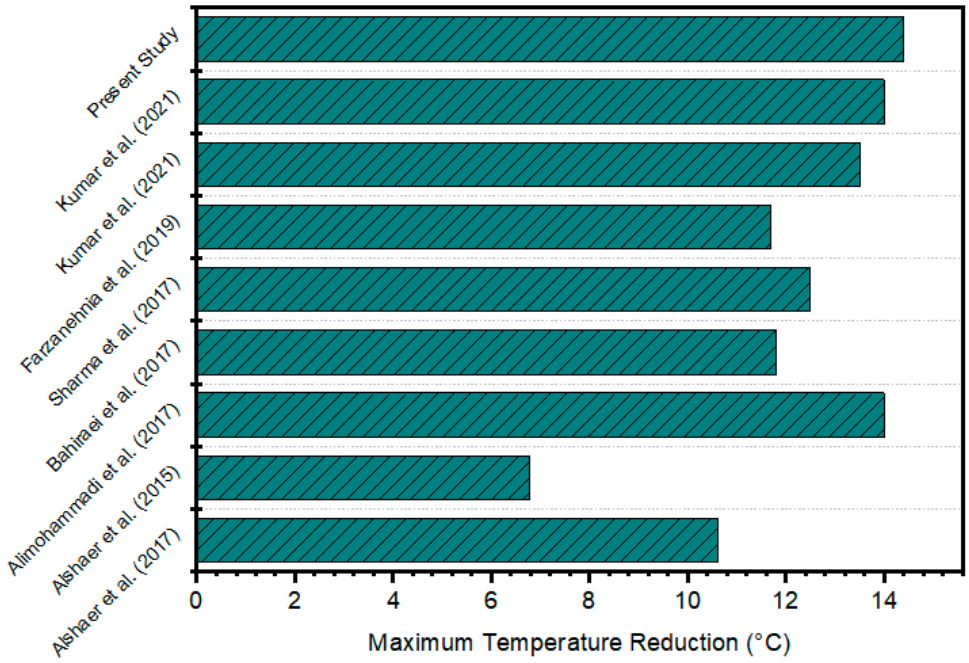

Figure 25. Thermal Management performance comparisons of the present study with the recent studies [11,34–40].

4. Conclusions

Thermal management of electronic equipment is crucial for optimal and efficient operation. The literature studies utilized pin fins, PCMs, NEPCMs, PCM/porous foams for thermal management analysis. The current experimental study is the first of its kind utilizing NEPCM along with copper foam for investigating the thermal management effectiveness of heat sink. The PCM used in the study was PT-58, and NPs of GNPs and MgO with 0.01 wt.% and 0.02 wt.% were utilized. The heating inputs utilized for thermal characterization were 0.77 kW/m^2, 1.54 kW/m^2, and 2.3 kW/m^2. The introduction of NPs and copper foam in PCM was intended to augment the thermal conductivity of PCM and improve the thermal responsiveness of heat sink. The important results drawn from the study are:

- From the baseline comparison of heat sink it is noticed that the G2-NEPCM/copper foam performed best among all configurations at all heating inputs. The reason is high thermal conductivity of GNPs, NPs and copper foam.
- The increase in NPs concentration in PCM improved the cooling capacity of heat sink and lowered the base temperature. For G2-NEPCM and M2-NEPCM, base temperature reduced by 8.03% and 7.6% at 0.77 kW/m^2, 9.1% and 8.3% at 1.54 kW/m^2, and 6.9% and 5.3% at 2.3 kW/m^2, respectively.
- The introduction of copper foam in NEPCM further lowered the base temperature and delayed the latent heating phase of PCM. In the case of G2-NEPCM/copper foam, maximum temperature reductions of 7.92 °C, 13.85 °C and 13.26 °C were observed at heating inputs of 0.77 kW/m^2, 1.54 kW/m^2 and 2.3 kW/m^2, respectively. While at 1.54 kW/m^2 and 2.3 kW/m^2 heating input, M2-NEPCM lowered the heat sink base temperature by 11.35 °C and 13.66 °C, which was better than all configurations. The reason was the NEPCM melting was not commenced in this case.
- Time required to achieve different target temperatures for various configurations of heat sink revealed that at 8 W power level, G2-NEPCM/copper foam took 64.4 min to reach 50 °C target temperature. While at 16 W power level, the G2-NEPCM/copper foam showed best performance and took 78 min in achieving target temperature of 70 °C. The M2-NEPCM/copper foam achieved target temperature of 70 °C in 74.8 min.

For 24 W power level, GNPs-NEPCM/copper foam took the highest time to achieve target temperatures of 50 °C, 60 °C, and 70 °C;

- The enhancement ratio study of heat sink indicated that dominance of NEPCM/copper foam-based heat sinks in general, and GNPs-NEPCM/copper foam specifically. The highest enhancement ratio of 5.8, 6.9 and 5.9 was observed for G2-NEPCM/copper foam at target temperatures of 50 °C, 60 °C and 70 °C, respectively, at 24 W power level.
- The overall cooling performance of heat sink was better in the case of NEPCM/copper foam composites as compared to PCM and NEPCM cases. The reason is that the copper foam helped to dissipate heat more uniformly and improved the heat transfer rate of PCM inside heat sink.
- The combined usage of NPs and metal foam is a good solution to mitigate the high heat load. The different types of NPs could have different influence on the thermal performance of PCM. The use of copper foam for thermal management exhibited better performance, even when simple PCM was used. The high thermal conductivity of copper foam improved the conduction and convection heat transfer in the PCM and NEPCM.

Author Contributions: Methodology, A.A. and F.J.; Formal analysis, F.H. and A.H.; Investigation, F.H.; Resources, A.H.; Writing—original draft, F.H.; Writing—review & editing, A.A. and F.J.; Supervision, A.H.; Conceptualization, H.M.A. All authors have read and agreed to the published version of the manuscript.

Funding: This research received no external funding.

Conflicts of Interest: The authors declare no conflict of interest.

Nomenclature

Abbreviations

Al_2O_3	Aluminium Oxide
CuO	Copper Oxide
GNPs	Graphene Nanoplatelets
Fe_2O_3	Iron Oxide
$Mn(NO_3)_2$	Magnesium Nitrate
MgO	Magnesium Oxide
min	Minute
MWCNTs	Multi Walled Carbon Nanotubes
NEPCM	Nano enriched PCM
NPs	Nanoparticles
PCM	Phase Change Materials
PPI	Pores Per Inch
TES	Thermal Energy Storage
TiO_2	Titanium Dioxide
TEM	Transmission Electron Microscopy
wt.%	Weight Percent

Symbols

k	Thermal conductivity (W/m.K)
P	Power (W)
q	Heating input (kW/m^2)
T_{max}	Maximum Temperature after Charging Phase (K)
V_{PCM}	Volume of PCM (mm^3)
I	Current (A)
L	Length of Heating Surface (mm)
W	Width of Heating Surface (mm)
m_{pcm}	Mass of PCM (g)
V_s	Volume of Heat Sink (mm^3)
T1–T8	Thermocouple Locations

V	Voltage (V)
T	Temperature (°C)
G	Thermal Conductance (W/k)
Greek Symbols	
ε	Porosity
ψ_{PCM}	Volume Fraction of PCM
ρ	Density
δ	Uncertainty Value
ξ	Enhancement Ratio in operation time
φ	Weight fraction of Nanoparticles

References

1. Hua, W.; Zhang, L.; Zhang, X. Research on Passive Cooling of Electronic Chips Based on PCM: A Review. *J. Mol. Liq.* **2021**, *340*, 117183. [CrossRef]
2. Sahoo, S.K.; Das, M.K.; Rath, P. Application of TCE-PCM Based Heat Sinks for Cooling of Electronic Components: A Review. *Renew. Sustain. Energy Rev.* **2016**, *59*, 550–582. [CrossRef]
3. Ghosh, D.; Ghose, J.; Datta, P.; Kumari, P.; Paul, S. Strategies for Phase Change Material Application in Latent Heat Thermal Energy Storage Enhancement: Status and Prospect. *J. Energy Storage* **2022**, *53*, 105179. [CrossRef]
4. Iradukunda, A.-C.; Vargas, A.; Huitink, D.; Lohan, D. Transient Thermal Performance Using Phase Change Material Integrated Topology Optimized Heat Sinks. *Appl. Therm. Eng.* **2020**, *179*, 115723. [CrossRef]
5. Mozafari, M.; Lee, A.; Mohammadpour, J. Thermal Management of Single and Multiple PCMs Based Heat Sinks for Electronics Cooling. *Therm. Sci. Eng. Prog.* **2021**, *23*, 100919. [CrossRef]
6. Kalbasi, R. Introducing a Novel Heat Sink Comprising PCM and Air—Adapted to Electronic Device Thermal Management. *Int. J. Heat Mass Transf.* **2021**, *169*, 120914. [CrossRef]
7. Xie, J.; Choo, K.F.; Xiang, J.; Lee, H.M. Characterization of Natural Convection in a PCM-Based Heat Sink with Novel Conductive Structures. *Int. Commun. Heat Mass Transf.* **2019**, *108*, 104306. [CrossRef]
8. Dammak, K.; El Hami, A. Thermal Reliability-Based Design Optimization Using Kriging Model of PCM Based Pin Fin Heat Sink. *Int. J. Heat Mass Transf.* **2021**, *166*, 120745. [CrossRef]
9. Sunku Prasad, J.; Anandalakshmi, R.; Muthukumar, P. Numerical Investigation on Conventional and PCM Heat Sinks under Constant and Variable Heat Flux Conditions. *Clean Technol. Environ. Policy* **2020**, *87*, 454–462. [CrossRef]
10. Cheng, P.; Chen, X.; Gao, H.; Zhang, X.; Tang, Z.; Li, A.; Wang, G. Different Dimensional Nanoadditives for Thermal Conductivity Enhancement of Phase Change Materials: Fundamentals and Applications. *Nano Energy* **2021**, *85*, 105948. [CrossRef]
11. Farzanehnia, A.; Khatibi, M.; Sardarabadi, M.; Passandideh-Fard, M. Experimental Investigation of Multiwall Carbon Nanotube/Paraffin Based Heat Sink for Electronic Device Thermal Management. *Energy Convers. Manag.* **2019**, *179*, 314–325. [CrossRef]
12. Fan, L.-W.; Zhu, Z.-Q.; Zeng, Y.; Xiao, Y.-Q.; Liu, X.-L.; Wu, Y.-Y.; Ding, Q.; Yu, Z.-T.; Cen, K.-F. Transient Performance of a PCM-Based Heat Sink with High Aspect-Ratio Carbon Nanofillers. *Appl. Therm. Eng.* **2015**, *75*, 532–540. [CrossRef]
13. Kothari, R.; Sahu, S.K.; Kundalwal, S.I. Investigation on Thermal Characteristics of Nano Enhanced Phase Change Material Based Finned and Unfinned Heat Sinks for Thermal Management System. *Chem. Eng. Process.-Process Intensif.* **2021**, *162*, 108328. [CrossRef]
14. Joseph, M.; Sajith, V. Graphene Enhanced Paraffin Nanocomposite Based Hybrid Cooling System for Thermal Management of Electronics. *Appl. Therm. Eng.* **2019**, *163*, 114342. [CrossRef]
15. Jalil, J.M.; Mahdi, H.S.; Allawy, A.S. Cooling Performance Investigation of PCM Integrated into Heat Sink with Nano Particles Addition. *J. Energy Storage* **2022**, *55*, 105466. [CrossRef]
16. Aramesh, M.; Shabani, B. Metal Foams Application to Enhance the Thermal Performance of Phase Change Materials: A Review of Experimental Studies to Understand the Mechanisms. *J. Energy Storage* **2022**, *50*, 104650. [CrossRef]
17. Marri, G.K.; Balaji, C. Experimental and Numerical Investigations on the Effect of Porosity and PPI Gradients of Metal Foams on the Thermal Performance of a Composite Phase Change Material Heat Sink. *Int. J. Heat Mass Transf.* **2021**, *164*, 120454. [CrossRef]
18. Venkateshwar, K.; Tasnim, S.H.; Simha, H.; Mahmud, S. Influence of Metal Foam Morphology on Phase Change Process under Temporal Thermal Load. *Appl. Therm. Eng.* **2020**, *180*, 115874. [CrossRef]
19. Li, W.; Zhang, D.; Jing, T.; Gao, M.; Liu, P.; He, G.; Qin, F. Nano-Encapsulated Phase Change Material Slurry (Nano-PCMS) Saturated in Metal Foam: A New Stable and Efficient Strategy for Passive Thermal Management. *Energy* **2018**, *165*, 743–751. [CrossRef]
20. Zhao, L.; Xing, Y.; Wang, Z.; Liu, X. The Passive Thermal Management System for Electronic Device Using Low-Melting-Point Alloy as Phase Change Material. *Appl. Therm. Eng.* **2017**, *125*, 317–327. [CrossRef]
21. Arshad, A.; Jabbal, M.; Faraji, H.; Talebizadehsardari, P.; Bashir, M.A.; Yan, Y. Thermal Performance of a Phase Change Material-Based Heat Sink in Presence of Nanoparticles and Metal-Foam to Enhance Cooling Performance of Electronics. *J. Energy Storage* **2022**, *48*, 103882. [CrossRef]

22. Lin, Y.; Jia, Y.; Alva, G.; Fang, G. Review on Thermal Conductivity Enhancement, Thermal Properties and Applications of Phase Change Materials in Thermal Energy Storage. *Renew. Sustain. Energy Rev.* **2018**, *82*, 2730–2742. [CrossRef]
23. Graphene Nanoplatelets (2–10 nm) Supplier—ACS Material. Available online: https://www.acsmaterial.com/graphene-nanoplatelets-2-10nm.html (accessed on 29 October 2021).
24. NanoAmor, Amorphous Products | Nanoscale Products | Nanopowder | Nanoparticles—Magnesium Oxide Nanopowder (MgO, 99+%, 20 Nm). Available online: https://www.nanoamor.com/inc/sdetail/2543 (accessed on 29 October 2021).
25. Ali, H.M.; Saieed, A.; Pao, W.; Ali, M. Copper Foam/PCMs Based Heat Sinks: An Experimental Study for Electronic Cooling Systems. *Int. J. Heat Mass Transf.* **2018**, *127*, 381–393.
26. Jamil, F.; Ali, H.M.; Nasir, M.A.; Karahan, M.; Janjua, M.M.; Naseer, A.; Ejaz, A.; Pasha, R.A. Evaluation of Photovoltaic Panels Using Different Nano Phase Change Material and a Concise Comparison: An Experimental Study. *Renew. Energy* **2021**, *169*, 1265–1279. [CrossRef]
27. Venugopal, J.; Prathap, L.; Rao, C.M.M.P.; Alagesan, J.; Manjunatha, L.H.; Gangodkar, D.; Mohanavel, V.; Sathyamurthy, R. Synthesis and Characterization of Paraffin Wax with Carbon Nanotubes and Magnesium Oxide. *Energy Rep.* **2022**, *8*, 313–320. [CrossRef]
28. Eanest Jebasingh, B.; Valan Arasu, A. A Comprehensive Review on Latent Heat and Thermal Conductivity of Nanoparticle Dispersed Phase Change Material for Low-Temperature Applications. *Energy Storage Mater.* **2020**, *24*, 52–74. [CrossRef]
29. Jurčević, M.; Nižetić, S.; Arıcı, M.; Ocłoń, P. Comprehensive Analysis of Preparation Strategies for Phase Change Nanocomposites and Nanofluids with Brief Overview of Safety Equipment. *J. Clean. Prod.* **2020**, *274*, 122963. [CrossRef]
30. Rehman, T.-; Ali, H.M. Thermal Performance Analysis of Metallic Foam-Based Heat Sinks Embedded with RT-54HC Paraffin: An Experimental Investigation for Electronic Cooling. *J. Therm. Anal. Calorim.* **2020**, *140*, 979–990. [CrossRef]
31. Kline, S.J. Describing Uncertainty in Single Sample Experiments. *Mech. Eng.* **1953**, *75*, 3–8.
32. Leong, K.Y.; Chew, S.P.; Gurunathan, B.A.; Ahmad, K.Z.K.; Ong, H.C. An Experimental Approach to Investigate Thermal Performance of Paraffin Wax and 1-Hexadecanol Based Heat Sinks for Cooling of Electronic System. *Int. Commun. Heat Mass Transf.* **2019**, *109*, 104365. [CrossRef]
33. Tariq, S.L.; Ali, H.M.; Akram, M.A.; Janjua, M.M. Experimental Investigation on Graphene Based Nanoparticles Enhanced Phase Change Materials (GbNePCMs) for Thermal Management of Electronic Equipment. *J. Energy Storage* **2020**, *30*, 101497. [CrossRef]
34. Alshaer, W.G.; Rady, M.A.; Nada, S.A.; Palomo Del Barrio, E.; Sommier, A. An Experimental Investigation of Using Carbon Foam–PCM–MWCNTs Composite Materials for Thermal Management of Electronic Devices under Pulsed Power Modes. *Heat Mass Transf.* **2017**, *53*, 569–579. [CrossRef]
35. Alshaer, W.G.; Nada, S.A.; Rady, M.A.; Del Barrio, E.P.; Sommier, A. Thermal Management of Electronic Devices Using Carbon Foam and PCM/Nano-Composite. *Int. J. Therm. Sci.* **2015**, *89*, 79–86. [CrossRef]
36. Alimohammadi, M.; Aghli, Y.; Alavi, E.S.; Sardarabadi, M.; Passandideh-Fard, M. Experimental Investigation of the Effects of Using Nano/Phase Change Materials (NPCM) as Coolant of Electronic Chipsets, under Free and Forced Convection. *Appl. Therm. Eng.* **2017**, *111*, 271–279. [CrossRef]
37. Bahiraei, F.; Fartaj, A.; Nazri, G.-A. Experimental and Numerical Investigation on the Performance of Carbon-Based Nanoenhanced Phase Change Materials for Thermal Management Applications. *Energy Convers. Manag.* **2017**, *153*, 115–128. [CrossRef]
38. Sharma, S.; Micheli, L.; Chang, W.; Tahir, A.A.; Reddy, K.S.; Mallick, T.K. Nano-Enhanced Phase Change Material for Thermal Management of BICPV. *Appl. Energy* **2017**, *208*, 719–733. [CrossRef]
39. Kumar, A.; Kothari, R.; Sahu, S.K.; Kundalwal, S.I. A Comparative Study and Optimization of Phase Change Material Based Heat Sinks for Thermal Management of Electronic Components. *J. Energy Storage* **2021**, *43*, 103224. [CrossRef]
40. Kumar, A.; Kothari, R.; Sahu, S.K.; Kundalwal, S.I. Thermal Performance of Heat Sink Using Nano-Enhanced Phase Change Material (NePCM) for Cooling of Electronic Components. *Microelectron. Reliab.* **2021**, *121*, 114144. [CrossRef]